

Supplementary information

Enhanced Molecular Networking Shows *Microbacterium* sp. V1 as a Factory of Antioxidant Proline-Rich Peptides

Giovanni Andrea Vitale ¹, Silvia Scarpato ^{2,3}, Alfonso Mangoni ², Maria Valeria D'Auria ², Gerardo Della Sala ^{1*} and Donatella de Pascale ^{1*}

¹ Department of Eco-Sustainable Marine Biotechnology, Stazione Zoologica Anton Dohrn, Via A.F. Acton, Molosiglio, 80133 Naples, Italy; giovanniandrea.vitale@szn.it (G.A.V.);

² Department of Pharmacy, University of Naples “Federico II”, 80131 Naples, Italy; silvia.scarpato@unina.it (S.S.); alfonso.mangoni@unina.it (A.M.); madaura@unina.it (M.V.D.)

³ GEOMAR Centre for Marine Biotechnology (GEOMAR-Biotech), Research Unit Marine Natural Products Chemistry, GEOMAR Helmholtz Centre for Ocean Research Kiel, Am Kiel-Kanal 44, 24106 Kiel, Germany

* Correspondence: gerardo.dellasala@szn.it (G.D.S.); donatella.depascale@szn.it (D.d.P.)

Table S1. Mzmine parameters adopted for MS data processing.

Figure S1. Positive ion mode HR-ESI mass spectrum of compound **1**.

Figure S2. HR-MS/MS spectrum of the [M+H]⁺ pseudomolecular ion of compound **1**.

Figure S3. ¹H-NMR spectrum of compound **1**, (700 MHz, CD₃OD).

Figure S4. ¹³C-NMR spectrum of compound **1**, (175 MHz, CD₃OD).

Figure S5. COSY spectrum of compound **1**, (700 MHz, CD₃OD).

Figure S6. TOCSY spectrum of compound **1**, (700 MHz, CD₃OD).

Figure S7. ROESY spectrum of compound **1**, (700 MHz, CD₃OD).

Figure S8. HSQC spectrum of compound **1**, (700 MHz, CD₃OD).

Figure S9. Band-selective HMBC spectrum of compound **1**, (700 MHz, CD₃OD).

Figure S10. HMBC spectrum of compound **1**, (700 MHz, CD₃OD).

Figure S11. Band-selective HMBC spectrum of compound **1**, (700 MHz, CD₃OD).

Figure S12. Band-selective HMBC spectrum of compound **1**, (700 MHz, CD₃OD).

Figure S13. Advanced Marfey's analysis of compound **1**.

Table S2. Full NMR data of compound **2**, (¹H 700 MHz, ¹³C 175 MHz, CD₃OD).

Figure S14. Positive ion mode HR-ESI mass spectrum of compound **2**.

Figure S15 HR-MS/MS spectrum of the [M+H]⁺ pseudomolecular ion of compound **2**.

Figure S16. ¹H-NMR spectrum of compound **2**, (600 MHz, CD₃OD).

Figure S17. COSY spectrum of compound **2**, (700 MHz, CD₃OD).

Figure S18. TOCSY spectrum of compound **2**, (700 MHz, CD₃OD).

Figure S19. HSQC spectrum of compound **2**, (600 MHz, CD₃OD).

Figure S20. HMBC spectrum of compound **2**, (600 MHz, CD₃OD).

Figure S21. HR-MS/MS spectrum of the [M+H]⁺ and [M+2H]²⁺ ions of compound **3**.

Figure S22. HR-MS/MS spectrum of the [M+H]⁺ and [M+2H]²⁺ ions of compound **4**.

Figure S23. (A) HR-MS/MS spectrum of the [M+H]⁺ pseudomolecular ion of compound **5**.

Figure S24. HR-MS/MS spectrum of the [M+H]⁺ and [M+2H]²⁺ ions of compound **6**.

Figure S25. HR-MS/MS spectrum of the $[M+H]^+$ and $[M+2H]^{2+}$ ions of compound **7**.

Figure S26. HR-MS/MS spectrum of the $[M+H]^+$ and $[M+2H]^{2+}$ ions of compound **8**.

Figure S27. HRMS spectra showing iron adducts of compounds **1** (A) and **2** (B).

Table S3. Ferric reducing antioxidant power assay results of compounds **1** and **2**.

Figure S28. Peptidases from *Microbacterium sp.* V1 annotated by using the bioinformatic tool Hotpep-protease.

Table S1. Mzmine parameters adopted for MS data processing.

Mass Detection		Join aligner	
MS1 Detection	5·10 ⁴	m/z tolerance (ppm)	15
MS2 Detection	1·10 ²	Weight for mass	50
ADAP Chromatogram builder			
Min group size in n° of scans	4	RT tolerance (min)	0.3
Group intensity threshold	5·10 ⁴	Weight for RT	50
Min highest intensity	5·10 ⁴	Peak filter	
m/z tolerance (ppm)	20	Keep only features with MSMS scan	V
Chromatogram deconvolution (Baseline cut-off)			
Min peak height	5·10 ⁴	Intensity tolerance	10%
Peak duration range (min)	0-3	m/z tolerance (ppm)	20
Baseline level	5·10 ⁴	RT tolerance (min)	0.5
m/z range for MS2 scan pairing (Da)	0.002		
RT range for MS2 scan pairing (min)	0.3		

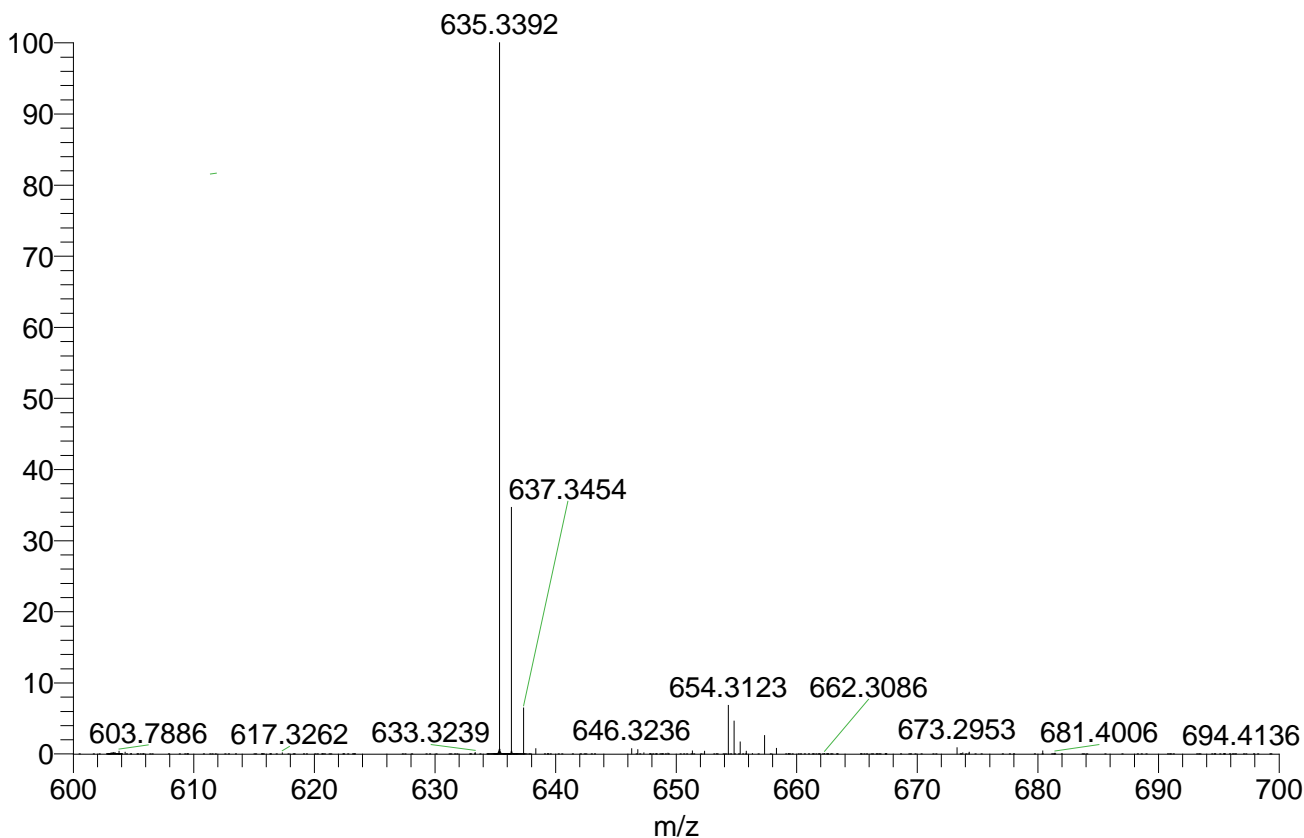


Figure S1. Positive ion mode HR-ESI mass spectrum of compound 1.

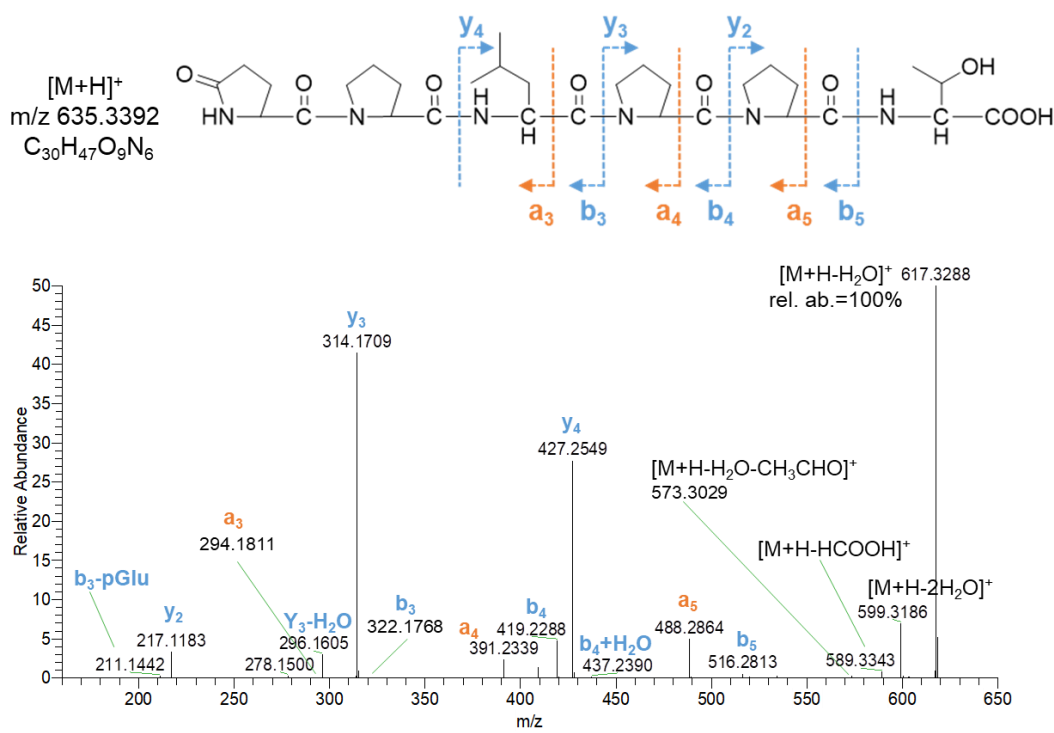


Figure S2. HR-MS/MS spectrum of the $[M+H]^+$ pseudomolecular ion of compound 1.

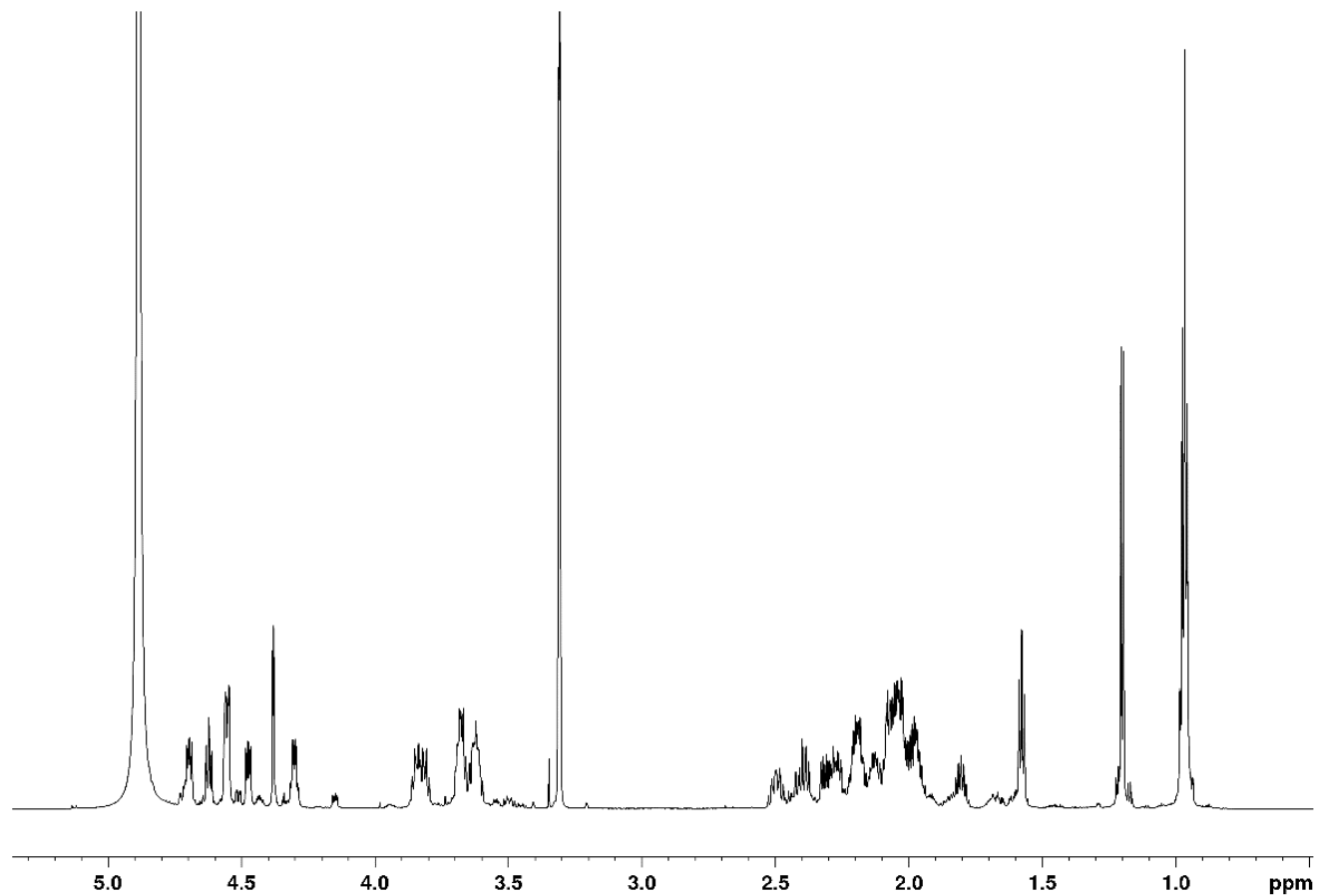


Figure S3. ¹H-NMR spectrum of compound 1 (700 MHz, CD₃OD).

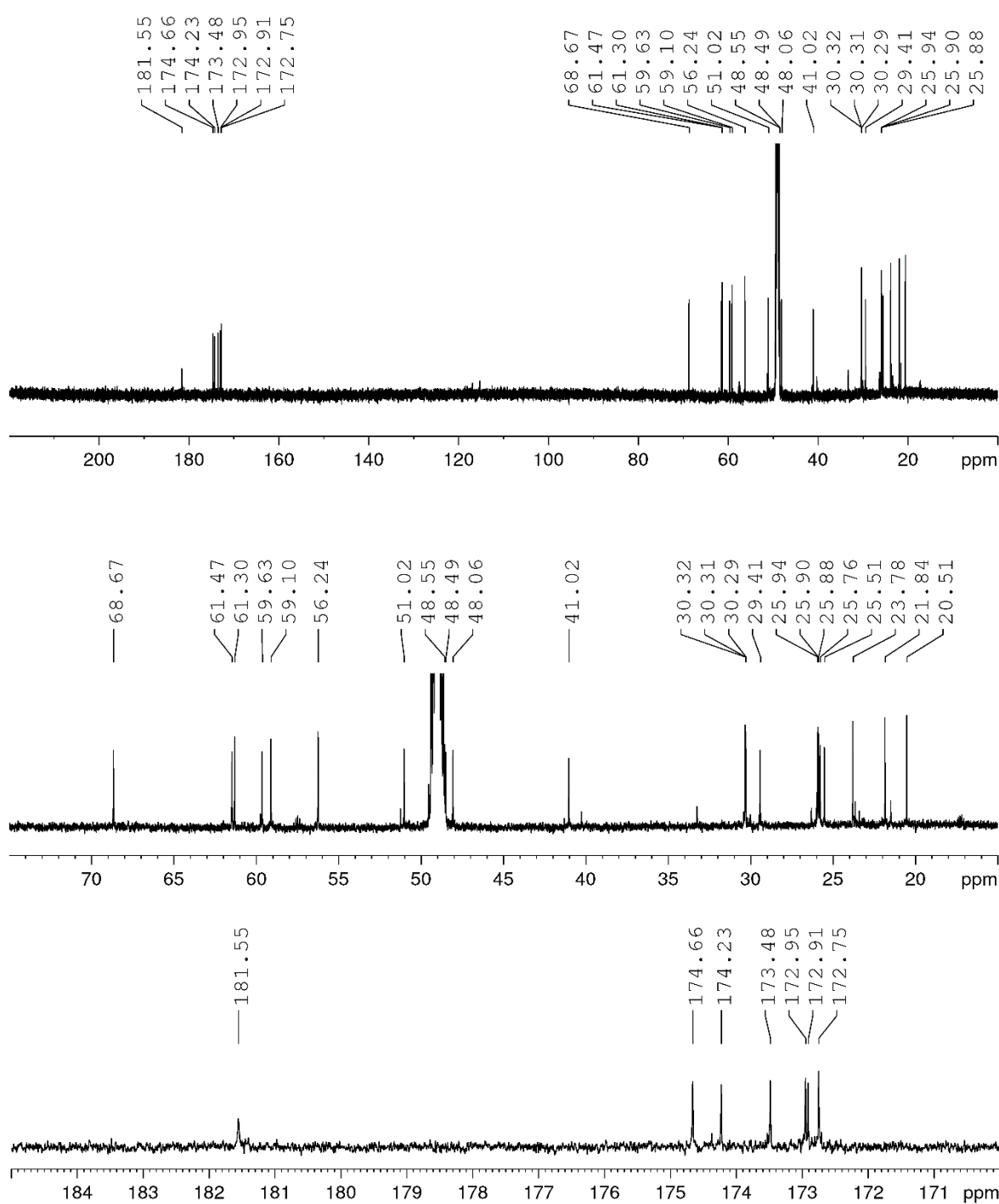
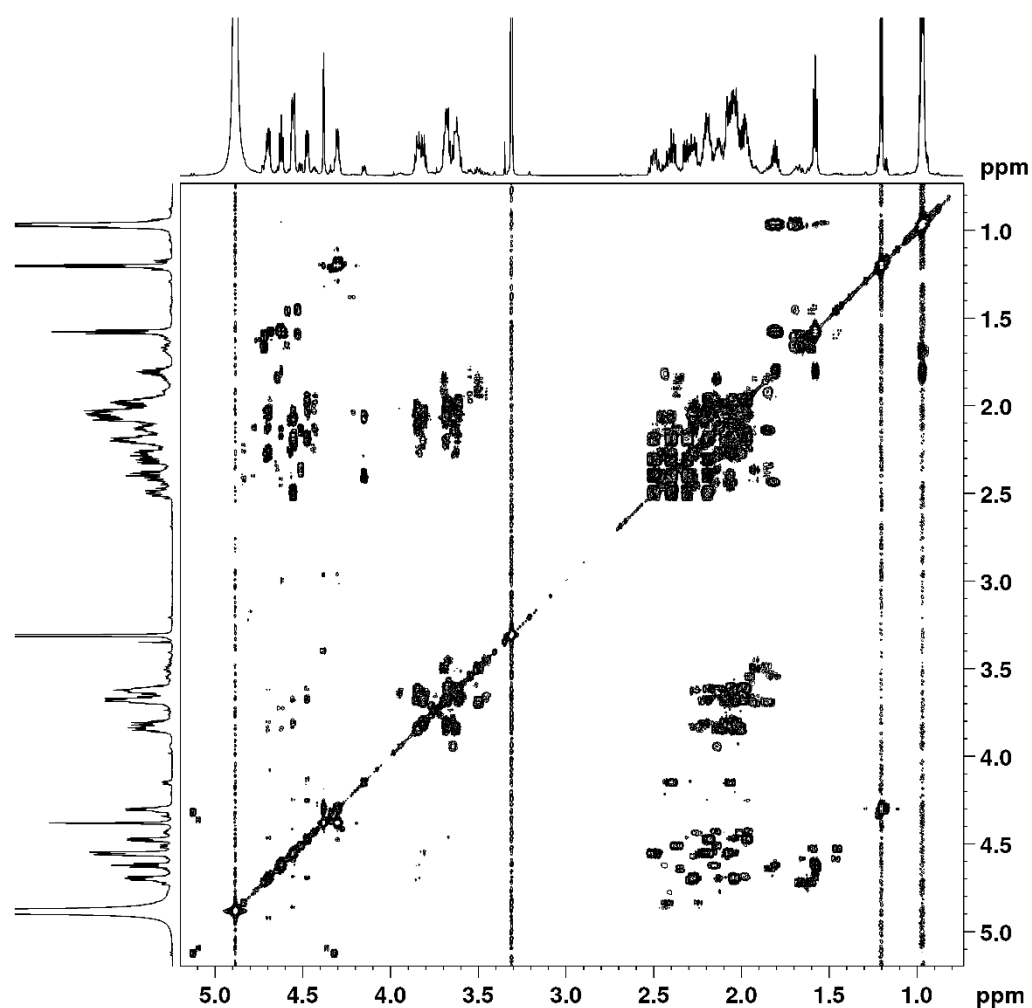


Figure S4. ^{13}C -NMR spectrum of compound 1 (175 MHz, CD_3OD).



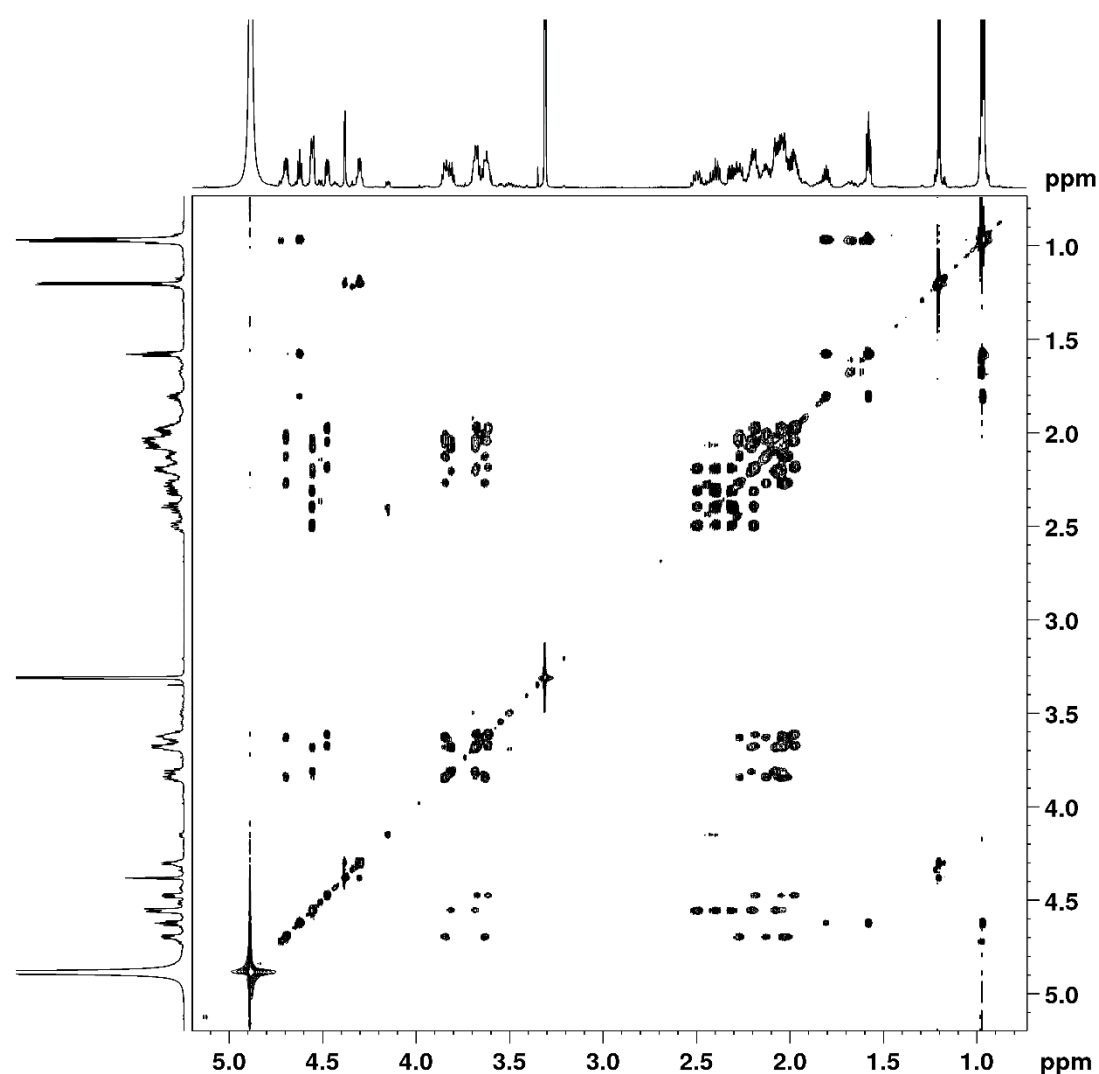


Figure S6. TOCSY spectrum of compound **1** (700 MHz, CD_3OD).

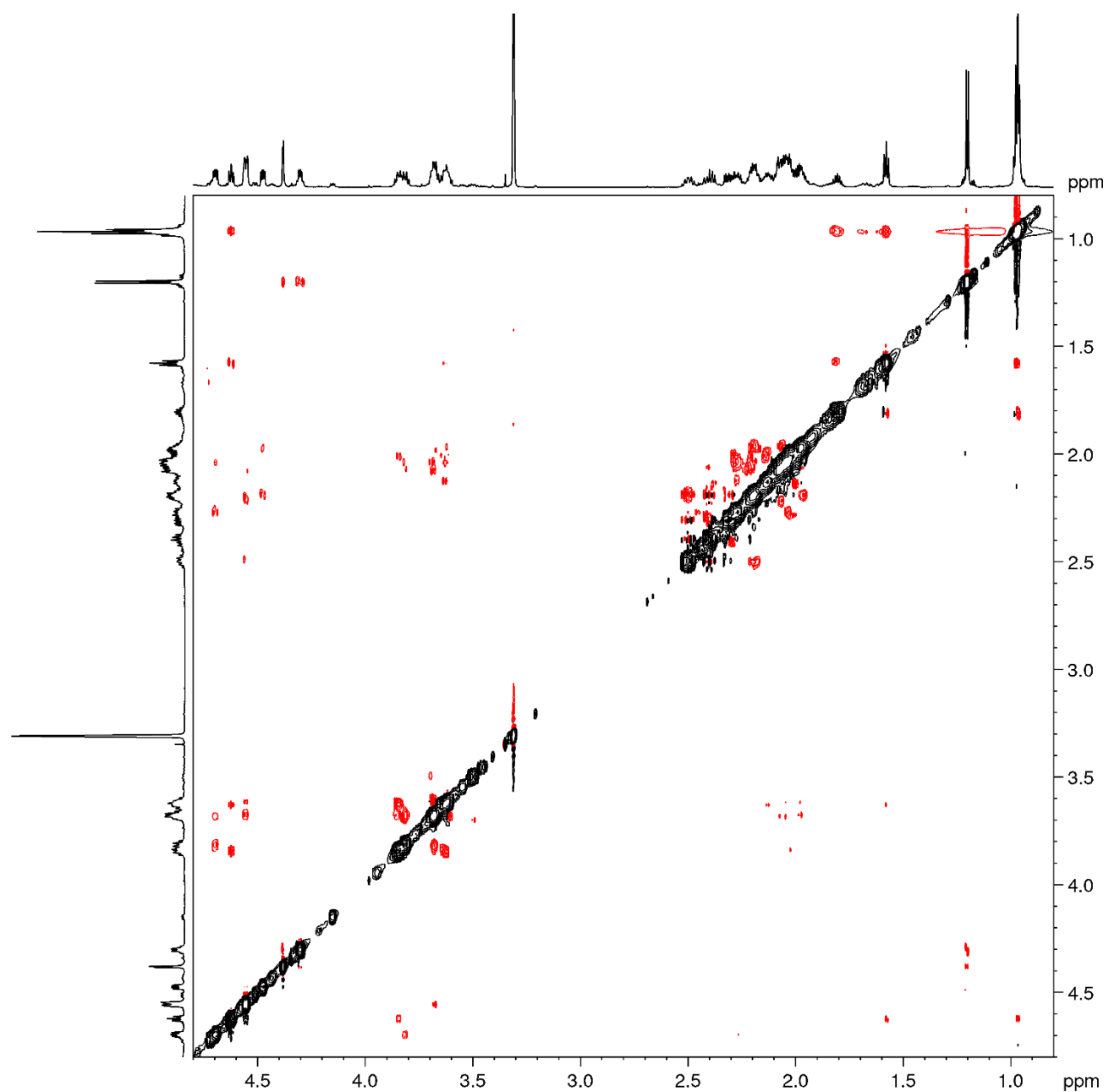


Figure S7. ROESY spectrum of compound **1** (**1**) (700 MHz, CD_3OD).

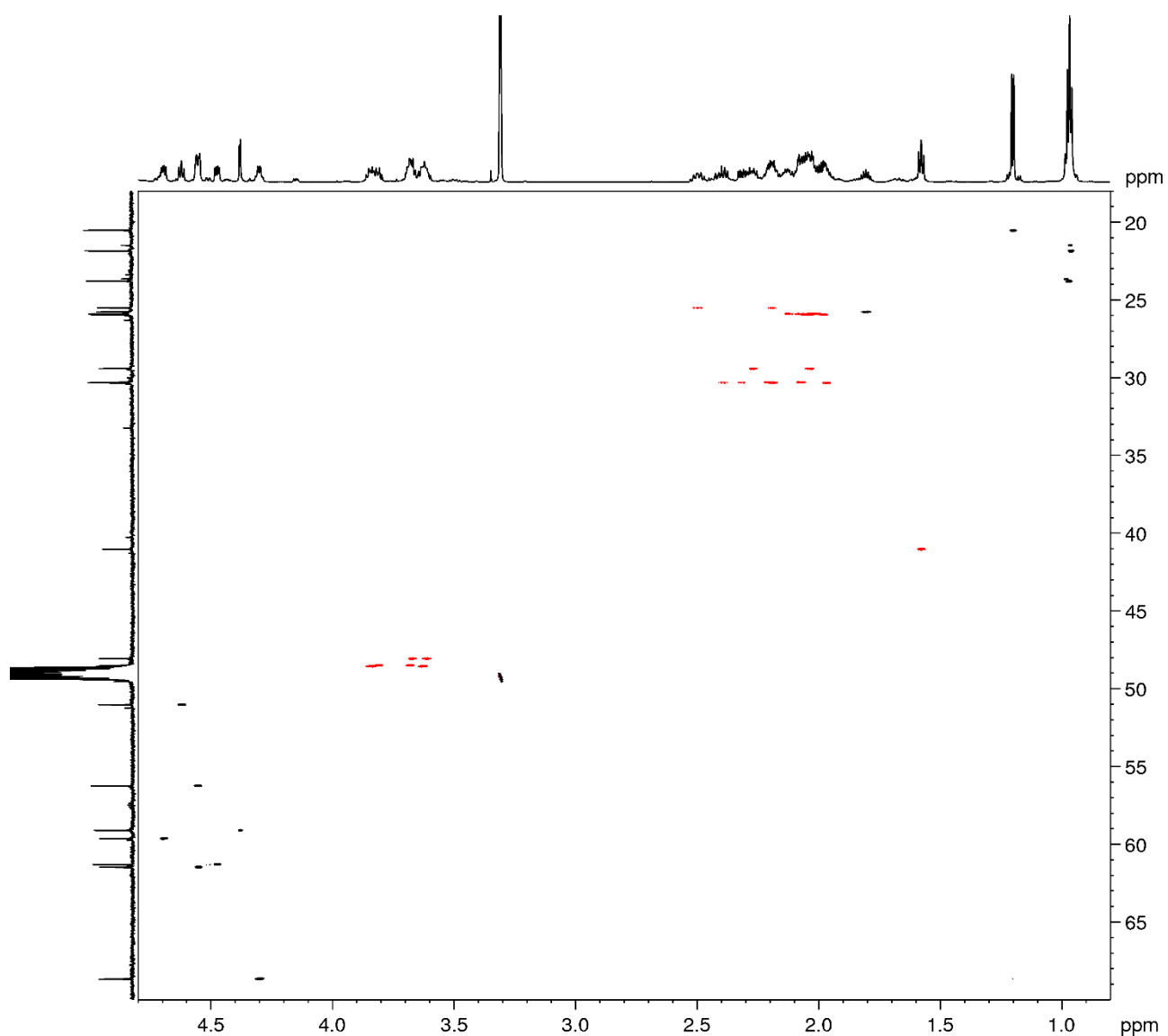


Figure S8. HSQC spectrum of compound **1** (700 MHz, CD_3OD).

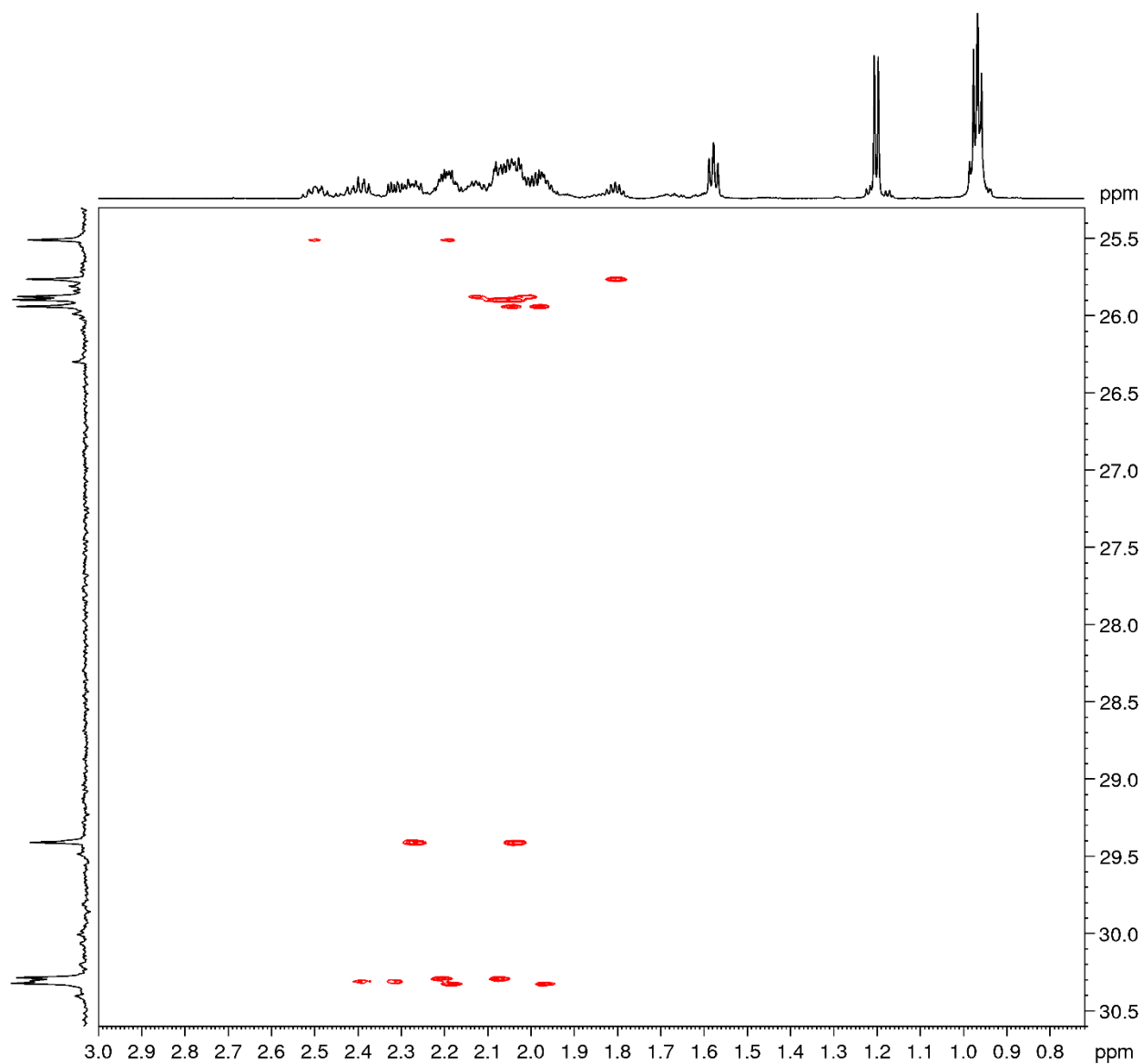


Figure S9. Band-selective HMBC spectrum of compound **1** (700 MHz, CD_3OD).

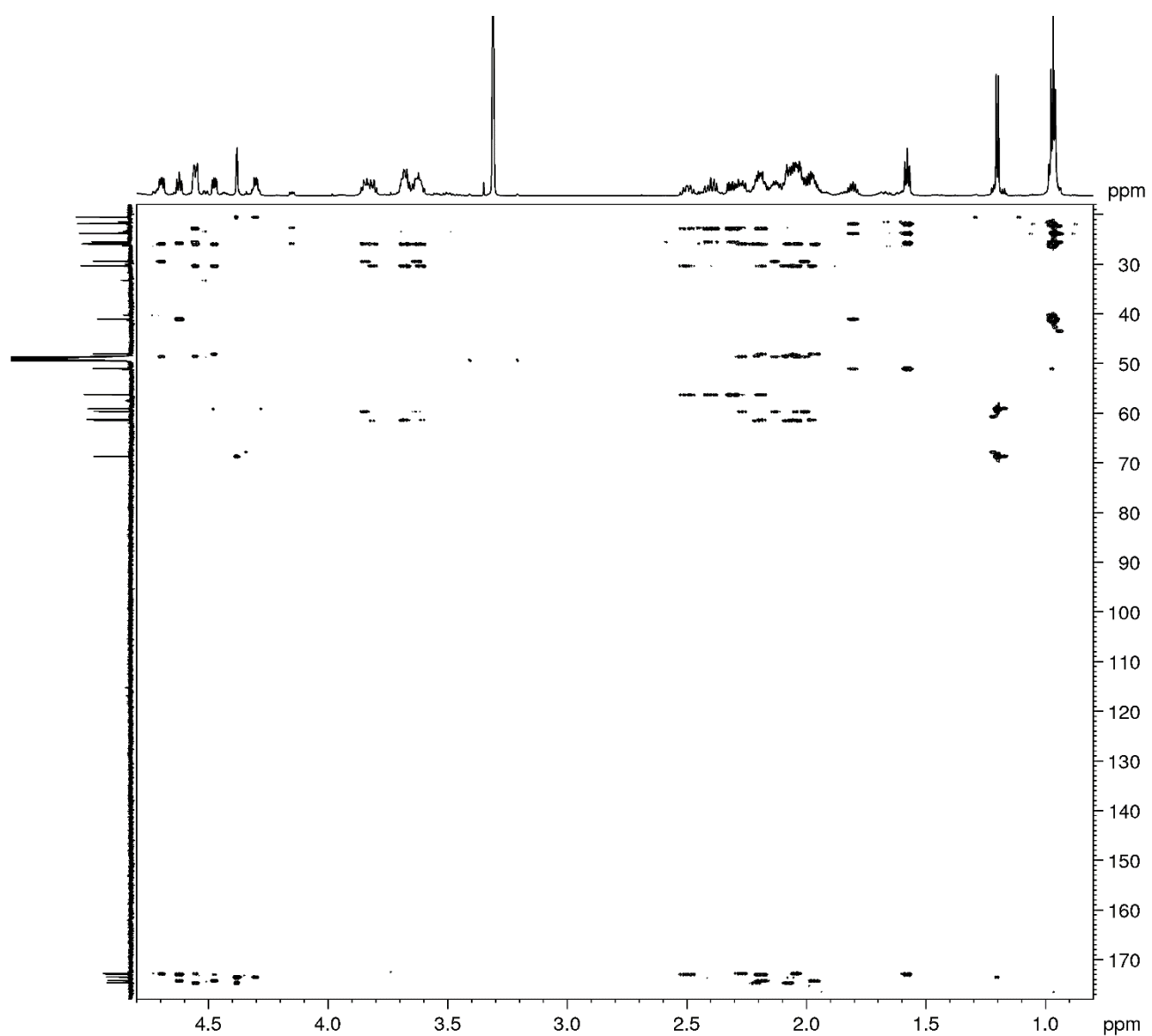


Figure S10. HMBC spectrum of compound **1** (700 MHz, CD₃OD).

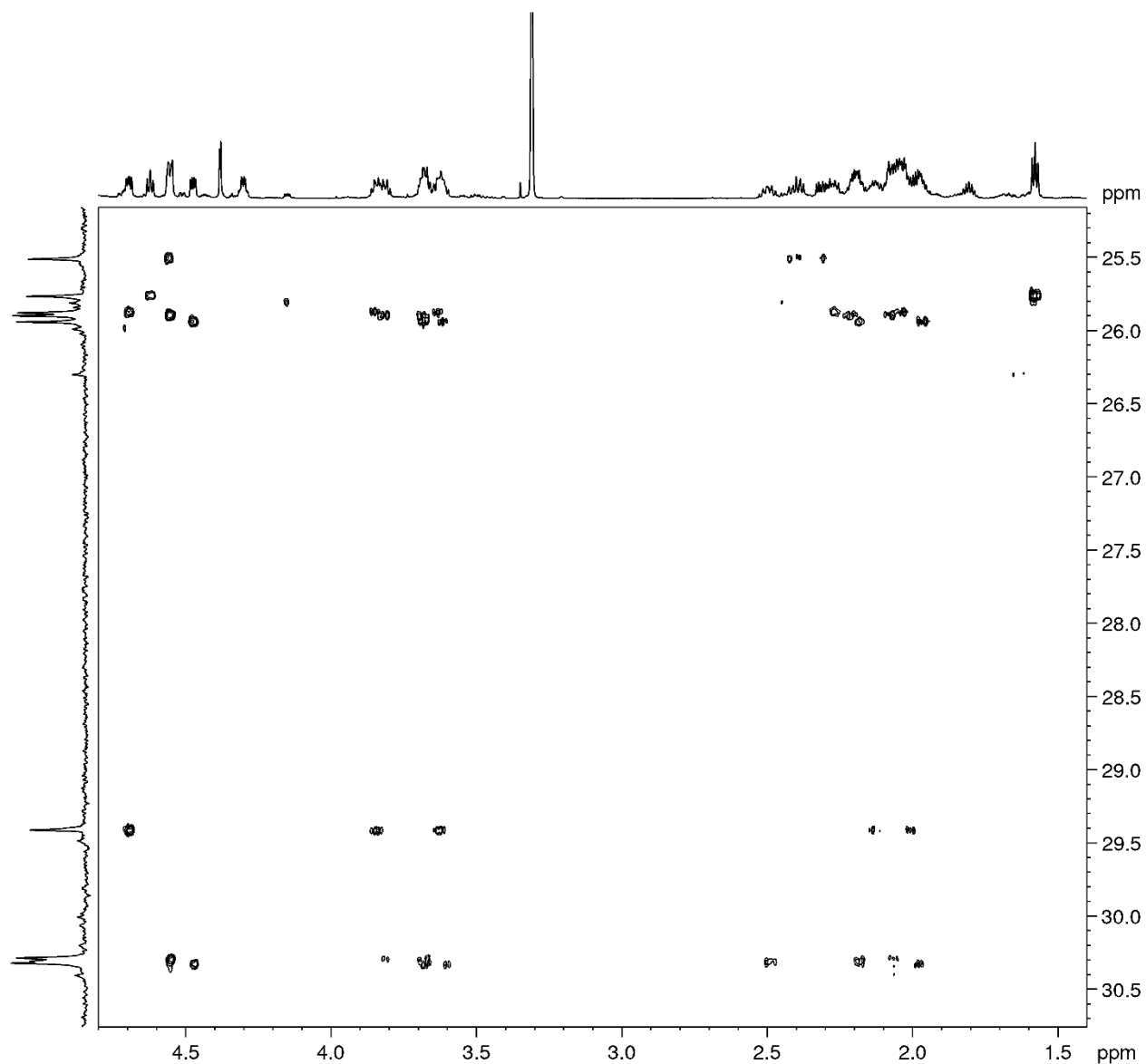


Figure S11. Band-selective HMBC spectrum of compound **1** (700 MHz, CD_3OD).

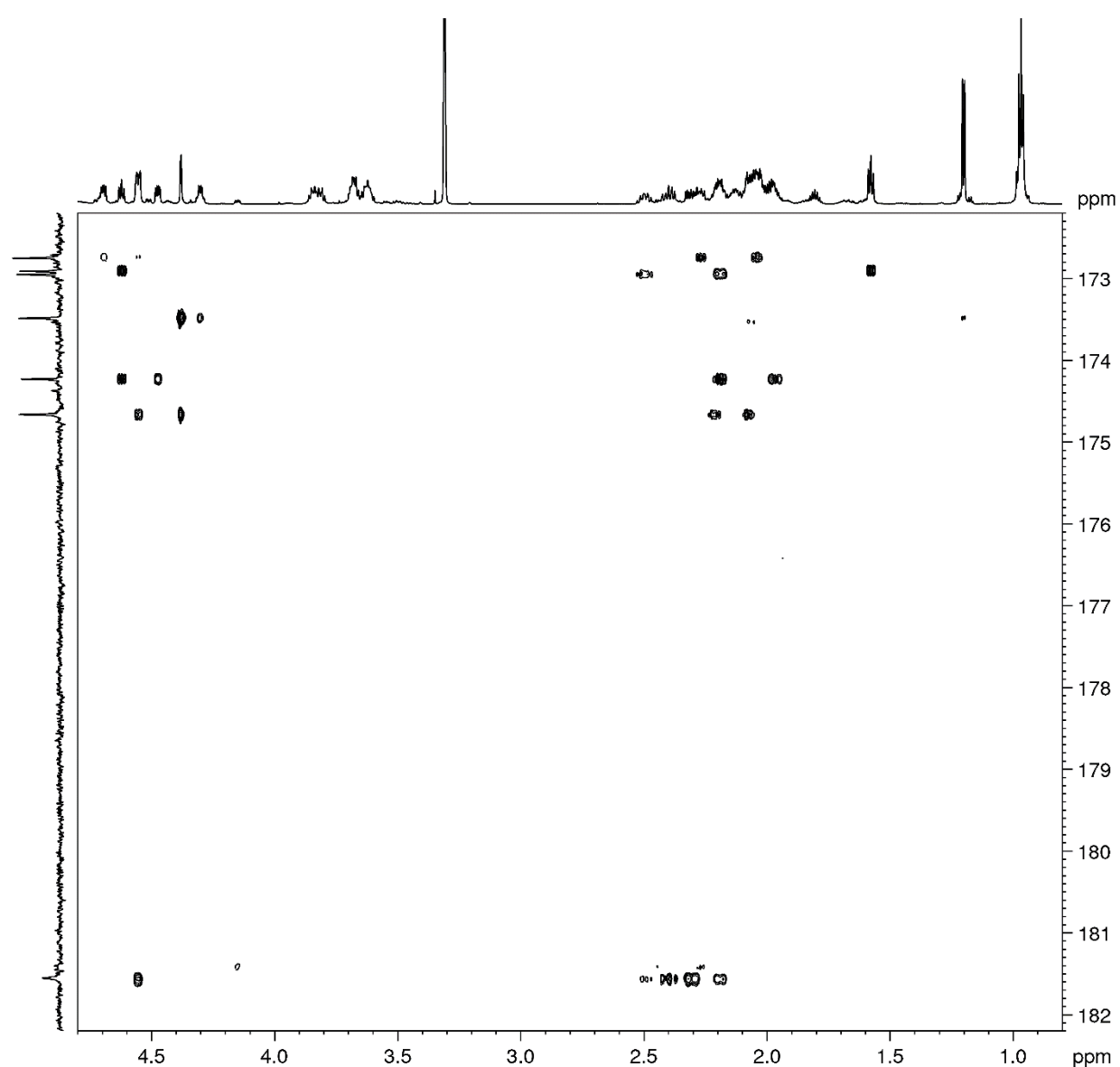


Figure S12. Band-selective HMBC spectrum of compound **1** (700 MHz, CD_3OD).

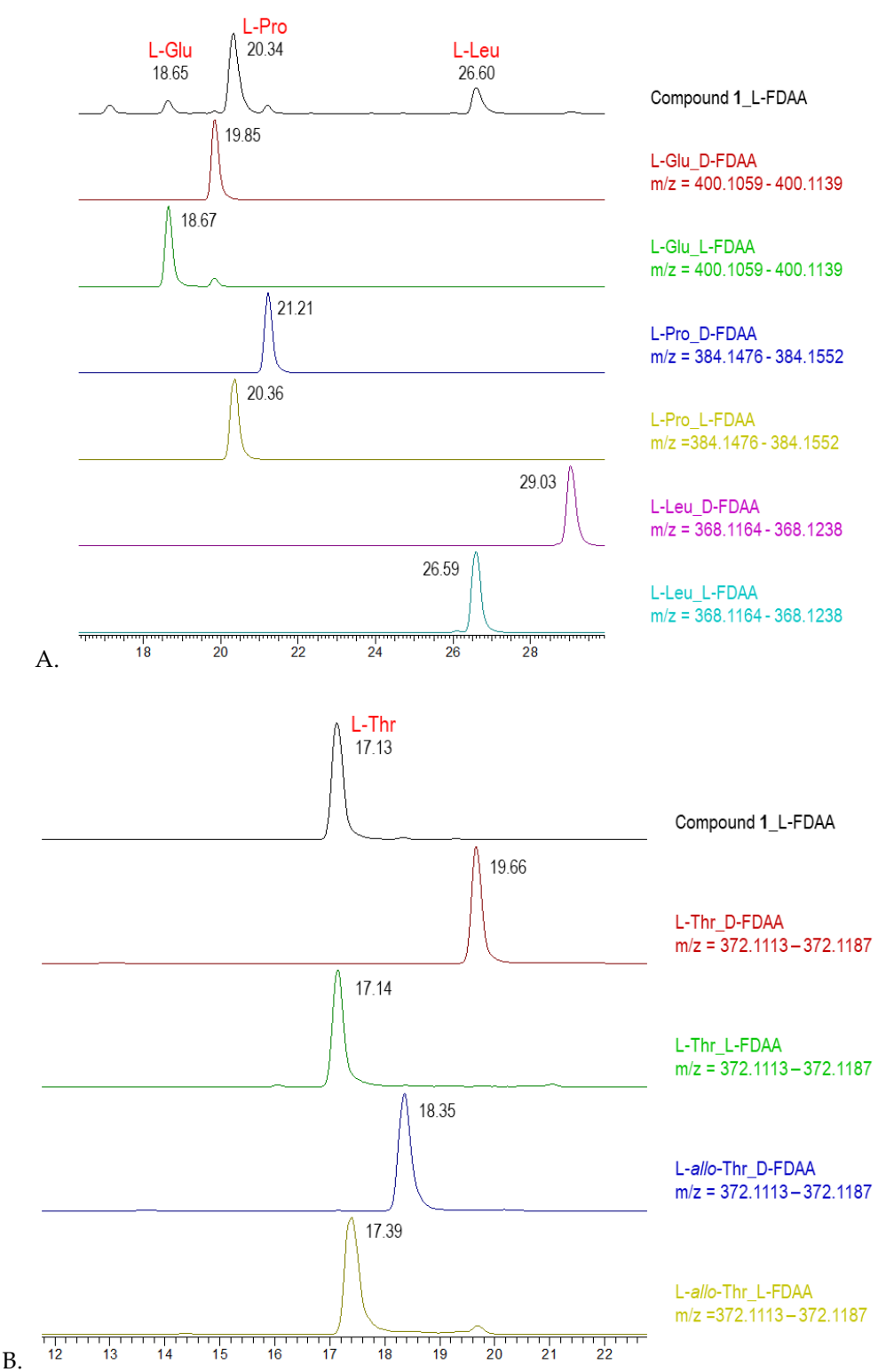


Figure S13. Advanced Marfey's analysis of compound **1**. Extracted-ion chromatograms at m/z 400.1099, at m/z 368.1201 and at m/z 384.1514 of the L-FDAA derivatives from the hydrolysis of **1** and of D- and L-FDAA derivatives L-Glu, L-Pro and L-Leu. (B) Extracted-ion chromatograms at m/z 372.1150 of the L-FDAA derivatives from the hydrolysis of **1** and of D- and L-FDAA derivatives L-Thr and L-*allo*-Thr.

Table S2. Full NMR data of compound **2** (¹H 600 MHz, ¹³C 175 MHz, CD₃OD).

AA	pos.	δ_C, type	δ_H, mult (J in Hz)	HMBC
pGlu	NH			
	1	172.99, C		
	2	56.25, CH	4.56, dd (4.2, 8.8)	pGlu-5
	3	25.58, CH ₂	a 2.50, m b 2.19, m	pGlu-1, pGlu-5 pGlu-1, pGlu-5
	4	30.38, CH ₂	a 2.40, m b 2.31, m	pGlu-5 pGlu-5
	5	181.55, C		
	1	174.5, C		
	2	61.37, CH	4.49, dd (4.3, 8.5)	Pro ^I -1
	3	30.36, CH ₂	a 2.18, m b 1.97, m	Pro ^I -1 Pro ^I -1
	4	25.94, CH ₂	a 2.03, m b 1.98, m	
	5	48.06, CH ₂	a 3.68, m b 3.61, m	
Leu	NH			
	1	173.03, C		
	2	51.14, CH	4.62, t (7.2)	Leu-1, Pro ^I -1
	3	41.12, CH ₂	1.57, t (7.2)	Leu-1
	4	25.86, CH	1.81, nonet (6.6)	
	5	21.92, CH ₃	0.96, d (6.6)	
Pro^{II}	1	172.70, C		
	2	59.67, CH	4.69 dd (4.5, 8.3)	Leu-1, Pro ^{II} -1
	3	29.19, CH ₂	a 2.27, m b 1.98, m	Pro ^{II} -1 Pro ^{II} -1
	4	25.87, CH ₂	a 2.13, m b 2.01, m	
	5	48.62, CH ₂	a 3.84, m b 3.65, m	
	1	175.46, C		
Pro^{III}	2	60.35, CH	4.44, m	Pro ^{II} -1, Pro ^{III} -1
	3	30.08, CH ₂	a 2.25, m b 2.00, m	Pro ^{III} -1 Pro ^{III} -1
	4	25.90, CH ₂	a 2.07, m b 2.04, m	
	5	48.50, CH ₂	a 3.80, m b 3.63, m	

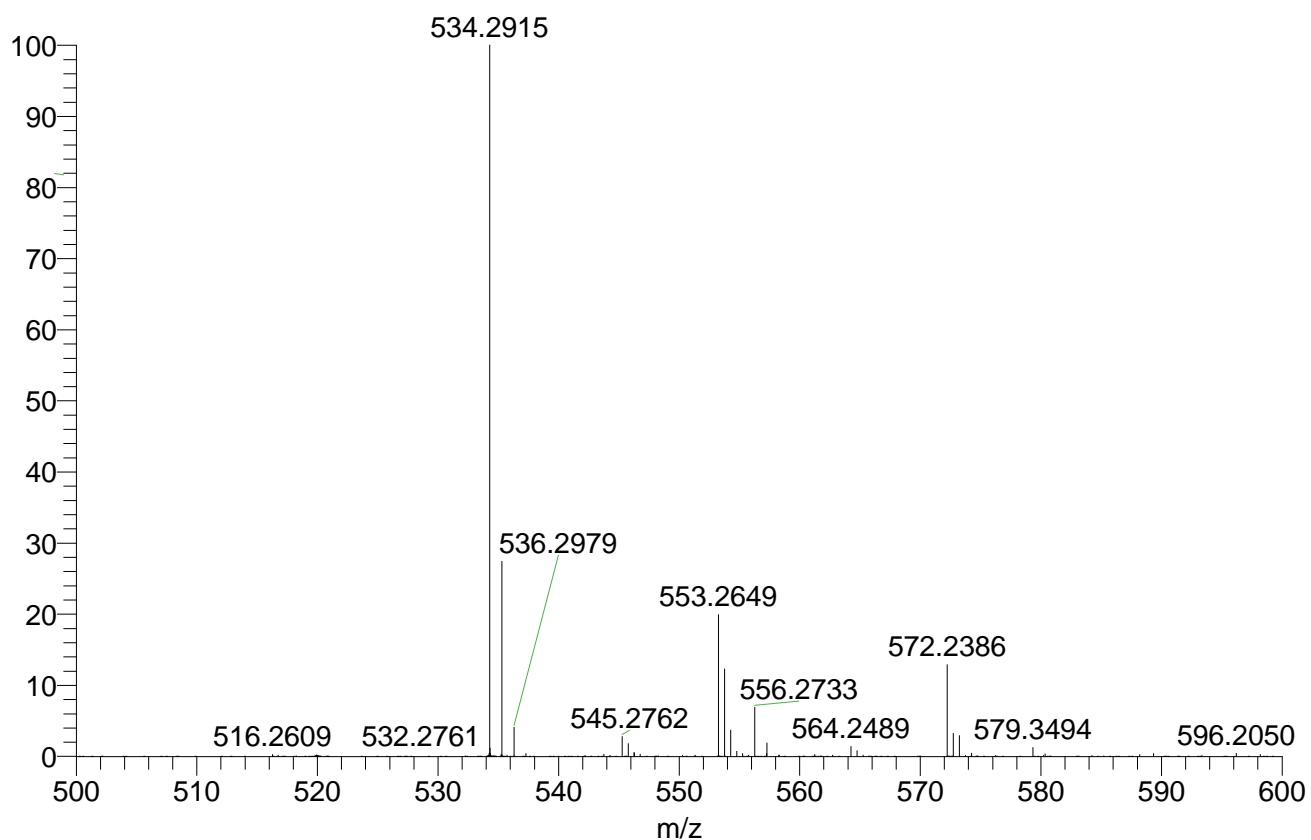


Figure S14. Positive ion mode HR-ESI mass spectrum of compound 2.

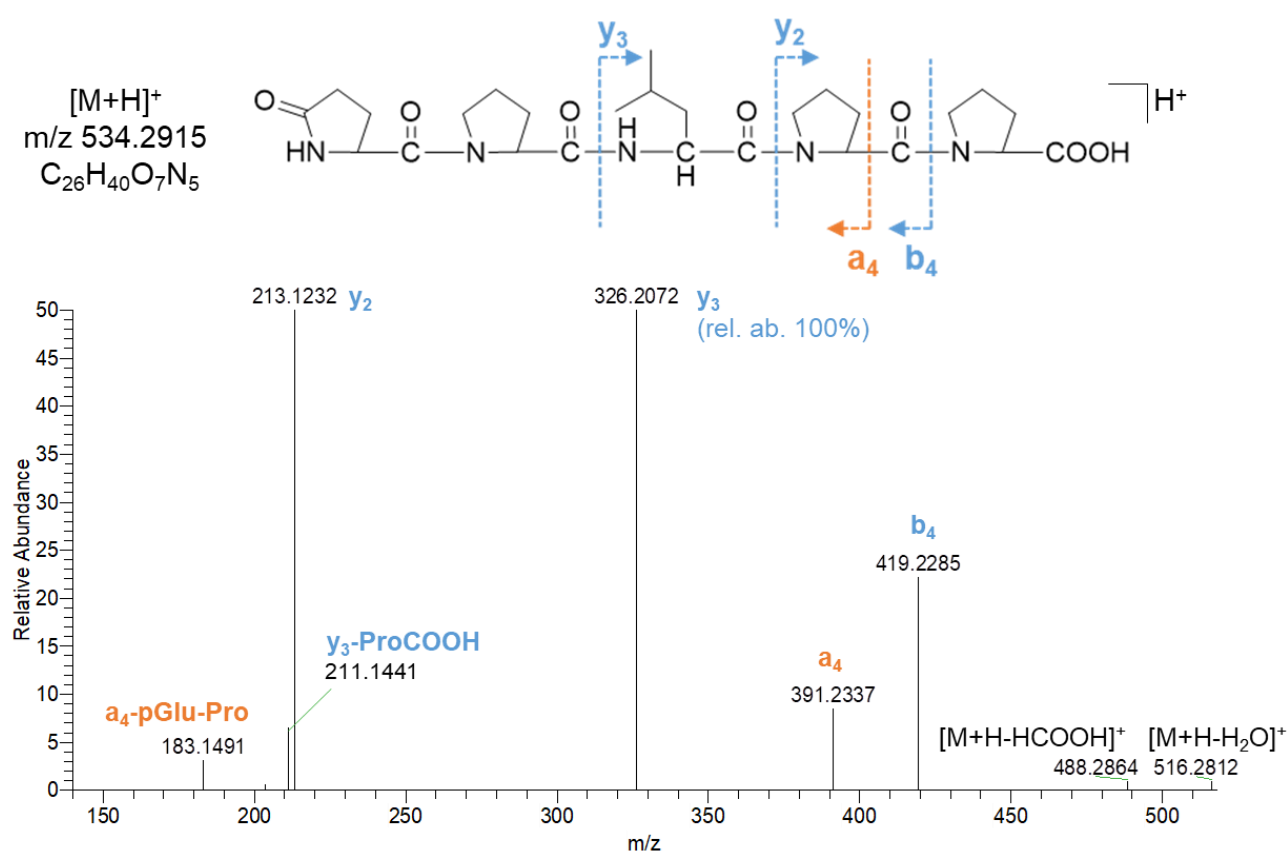


Figure S15. HR-MS/MS spectrum of the [M+H]⁺ pseudomolecular ion of compound 2.

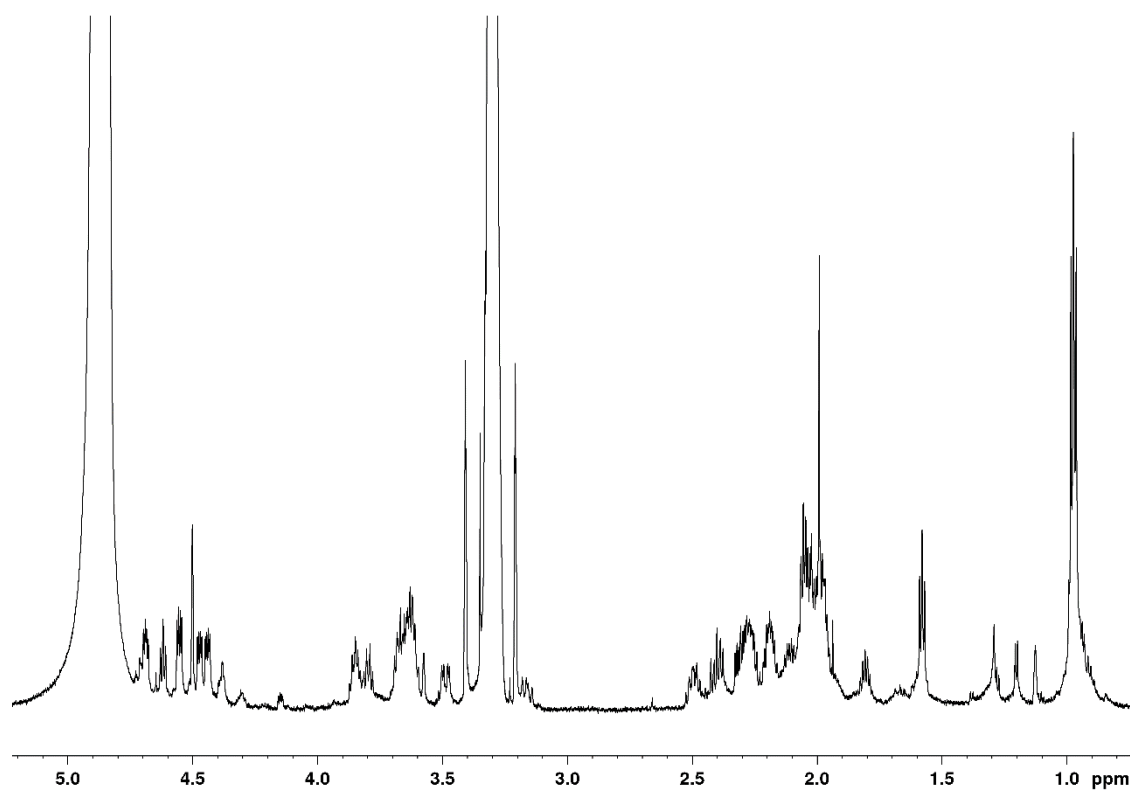


Figure S16. ¹H-NMR spectrum of compound **2** (700 MHz, CD₃OD).

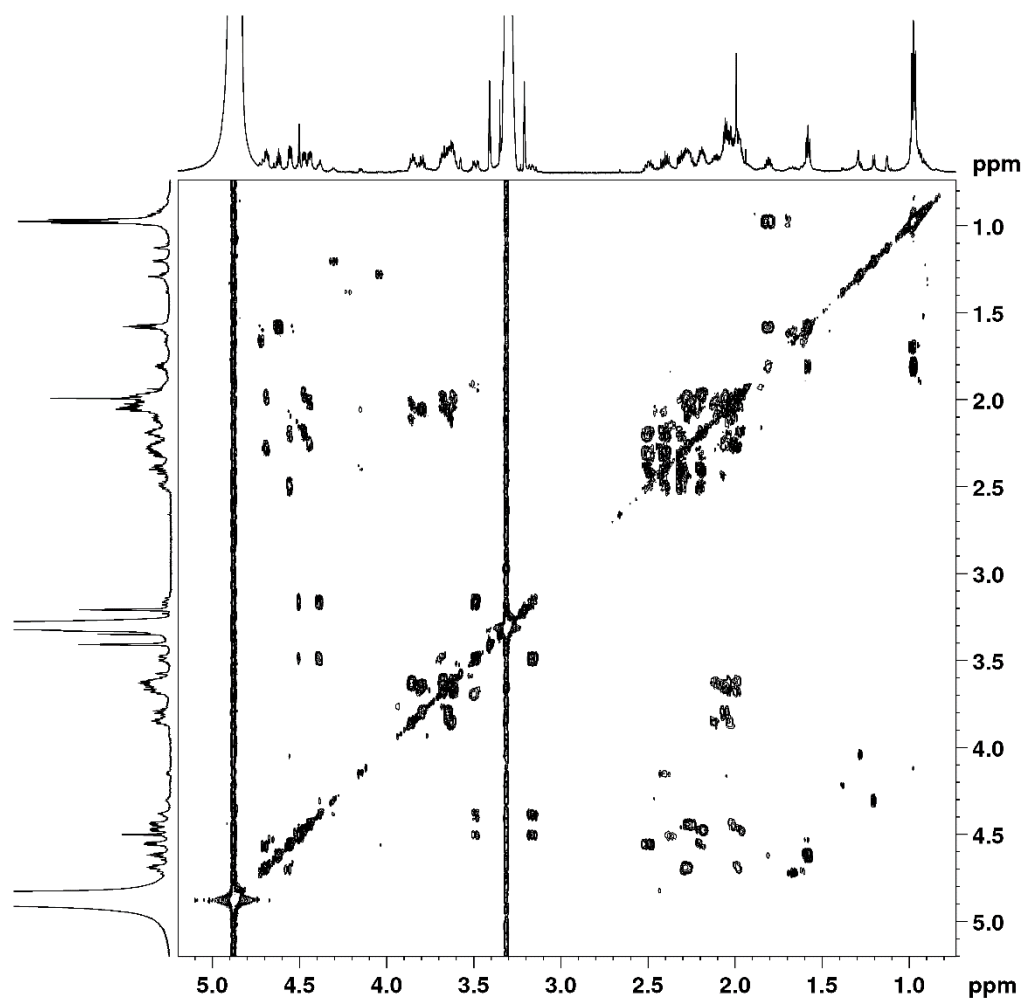


Figure S17. COSY spectrum of compound 2 (700 MHz, CD_3OD).

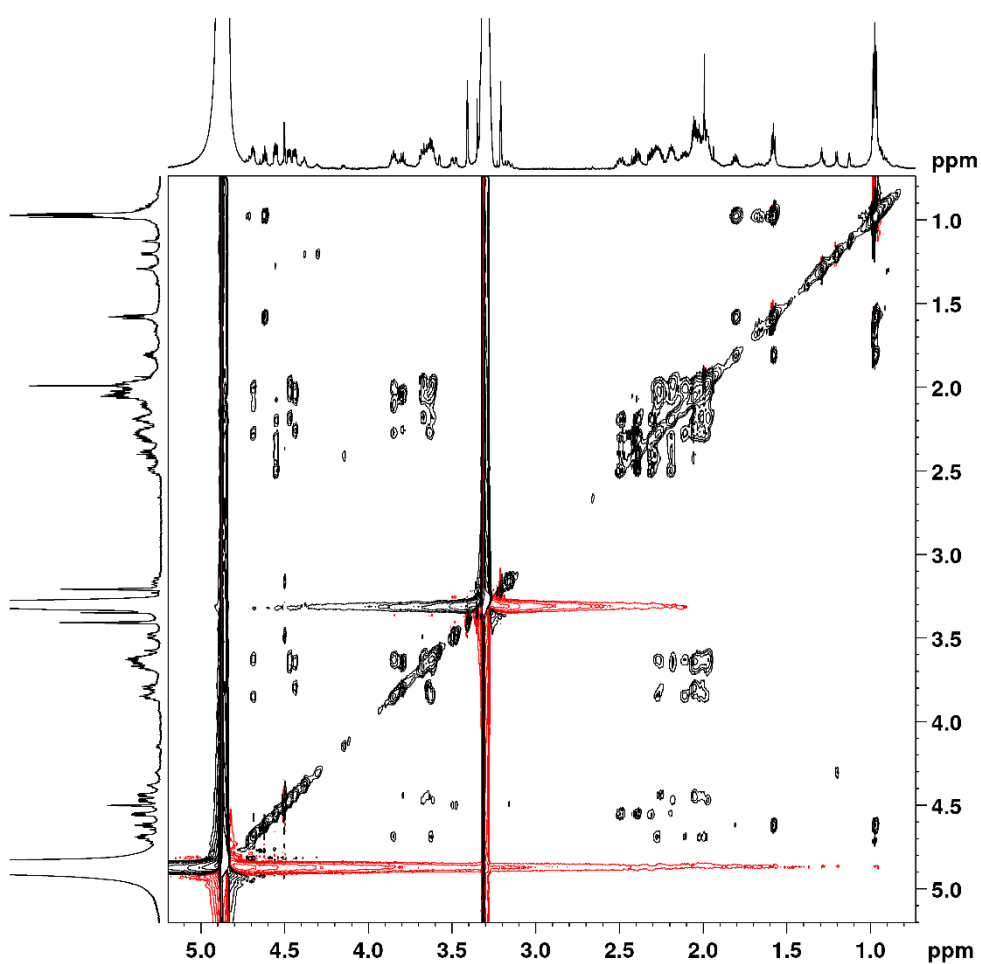


Figure S18. TOCSY spectrum of compound **2** (700 MHz, CD_3OD).

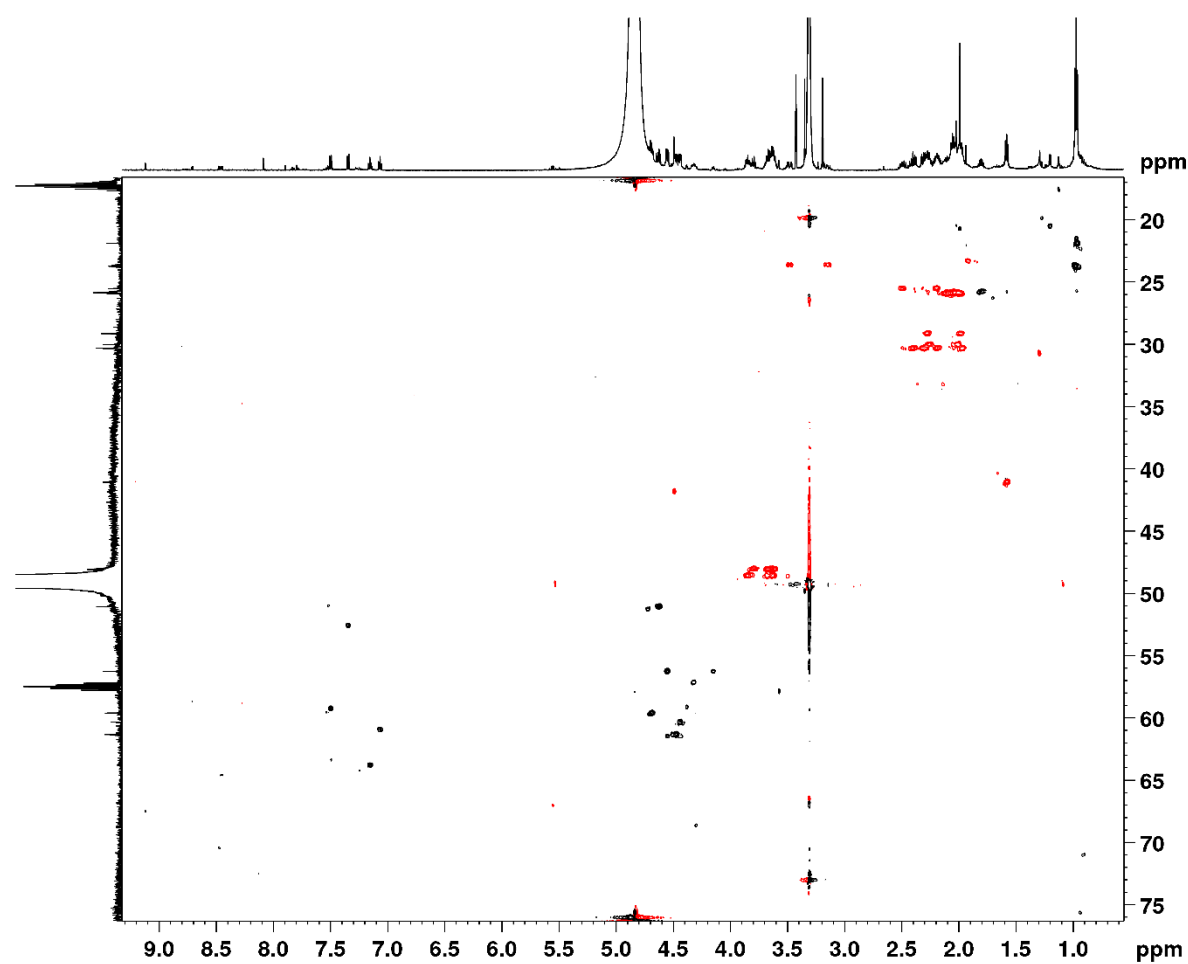


Figure S19. HSQC spectrum of compound **2** (600 MHz, CD_3OD).

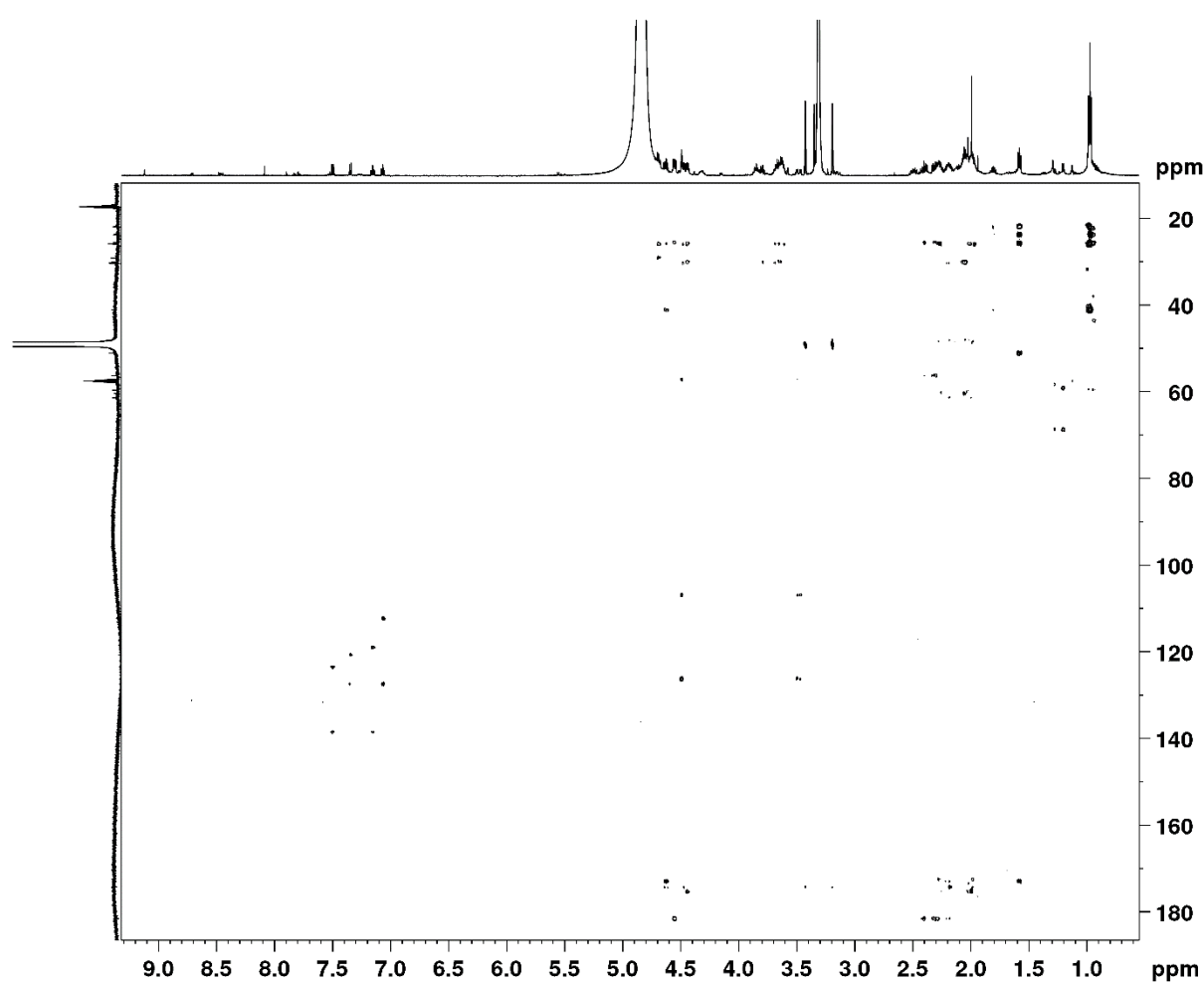


Figure S20. HMBC spectrum of compound 2 (600 MHz, CD_3OD).

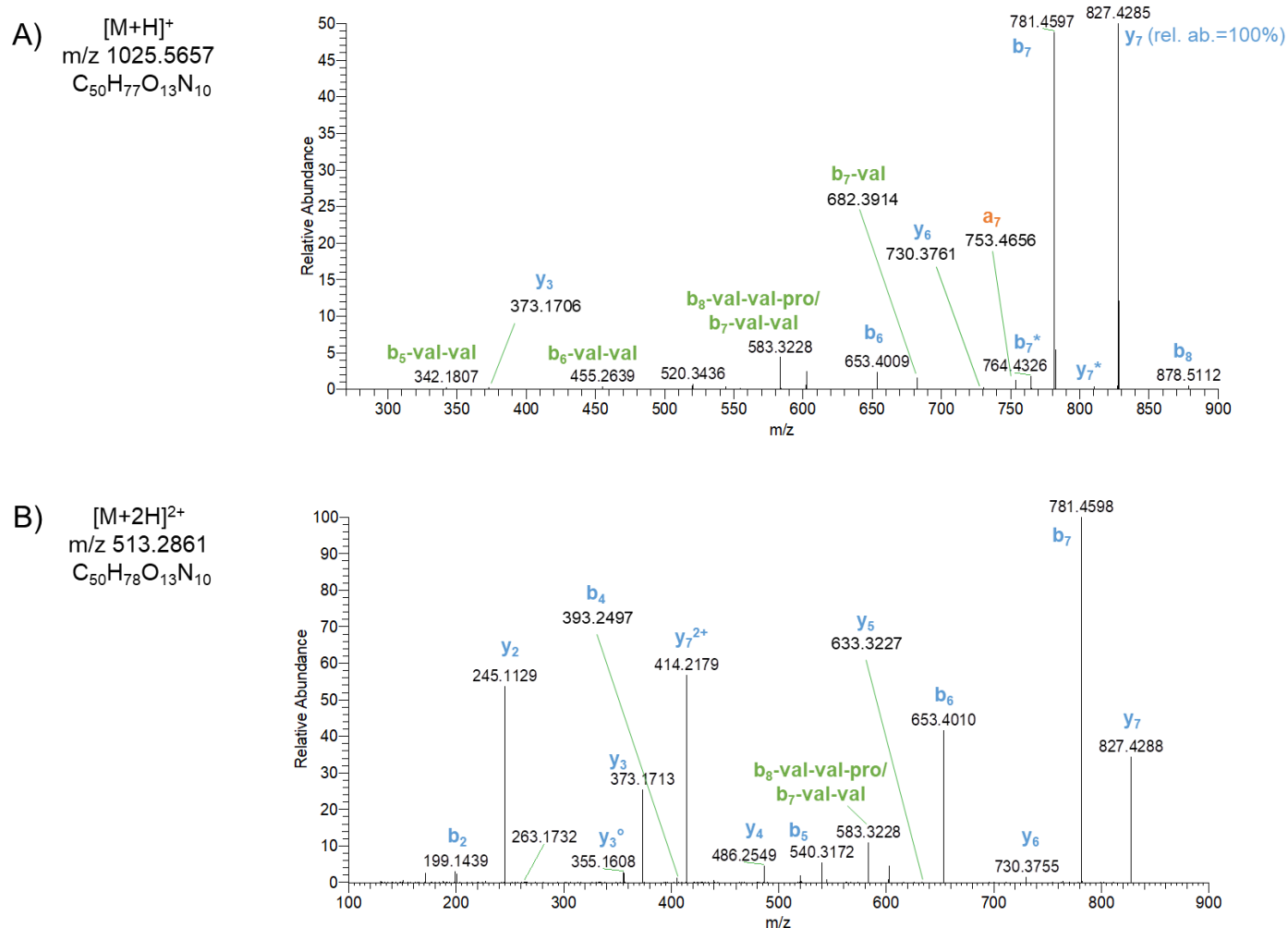
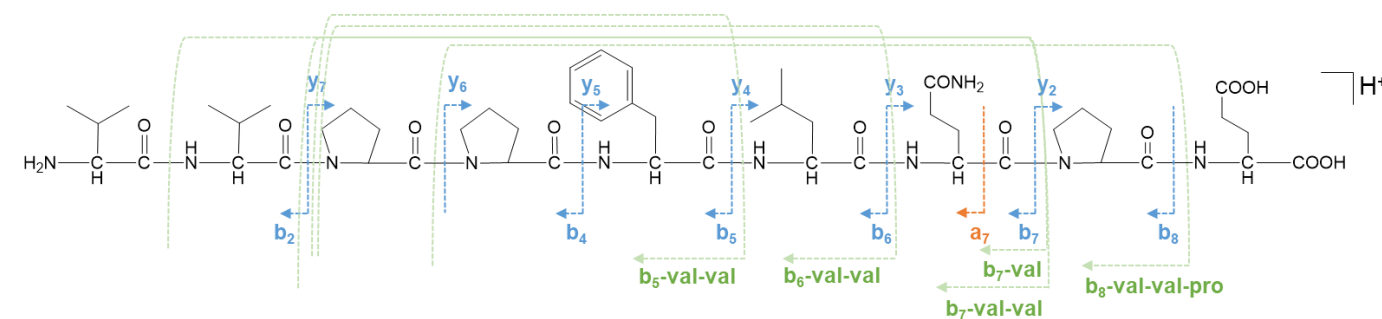


Figure S21. HR-MS/MS spectrum of the $[M+H]^+$ and $[M+2H]^{2+}$ ions of compound 3 ($R_t = 17.3$ min). Ions marked with a circle (°) derive from the corresponding fragment after water loss; ions marked with an asterisk (*) derive from the corresponding fragment after NH_3 loss.

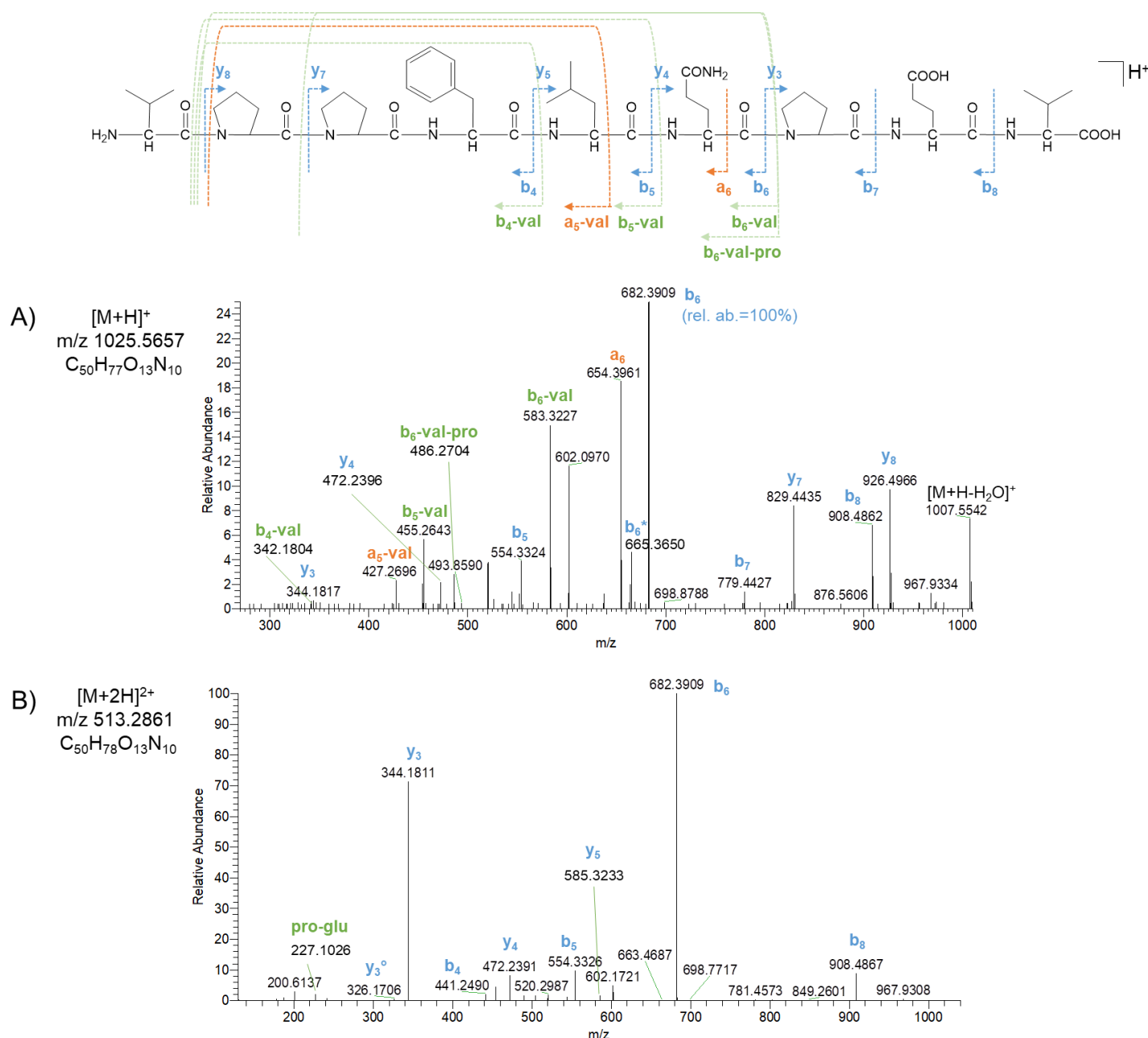


Figure S22. HR-MS/MS spectrum of the $[M+H]^+$ and $[M+2H]^{2+}$ ions of compound 4 ($R_t = 18.4$ min). Ions marked with a circle (\circ) derive from the corresponding fragment after water loss; ions marked with an asterisk (*) derive from the corresponding fragment after NH_3 loss.

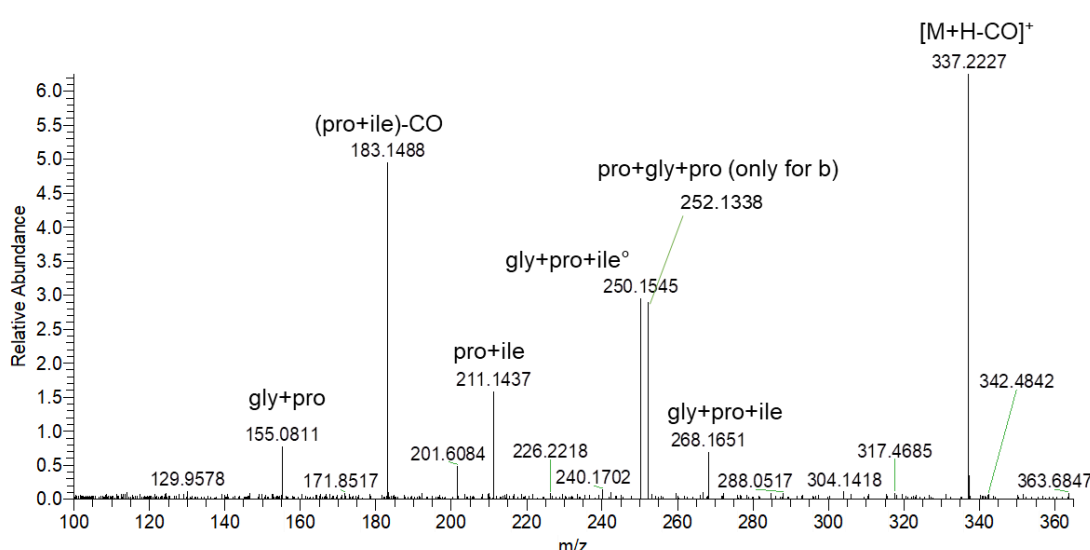
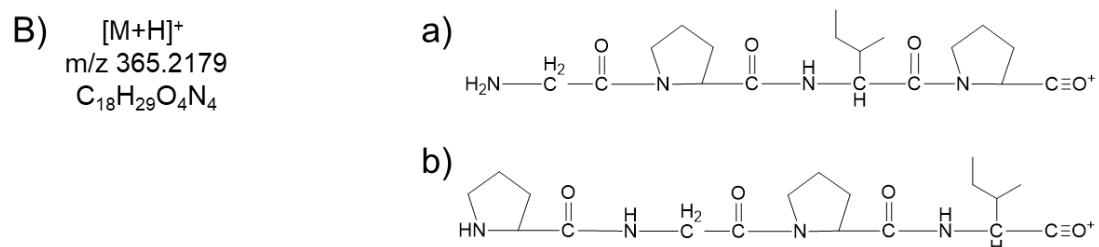
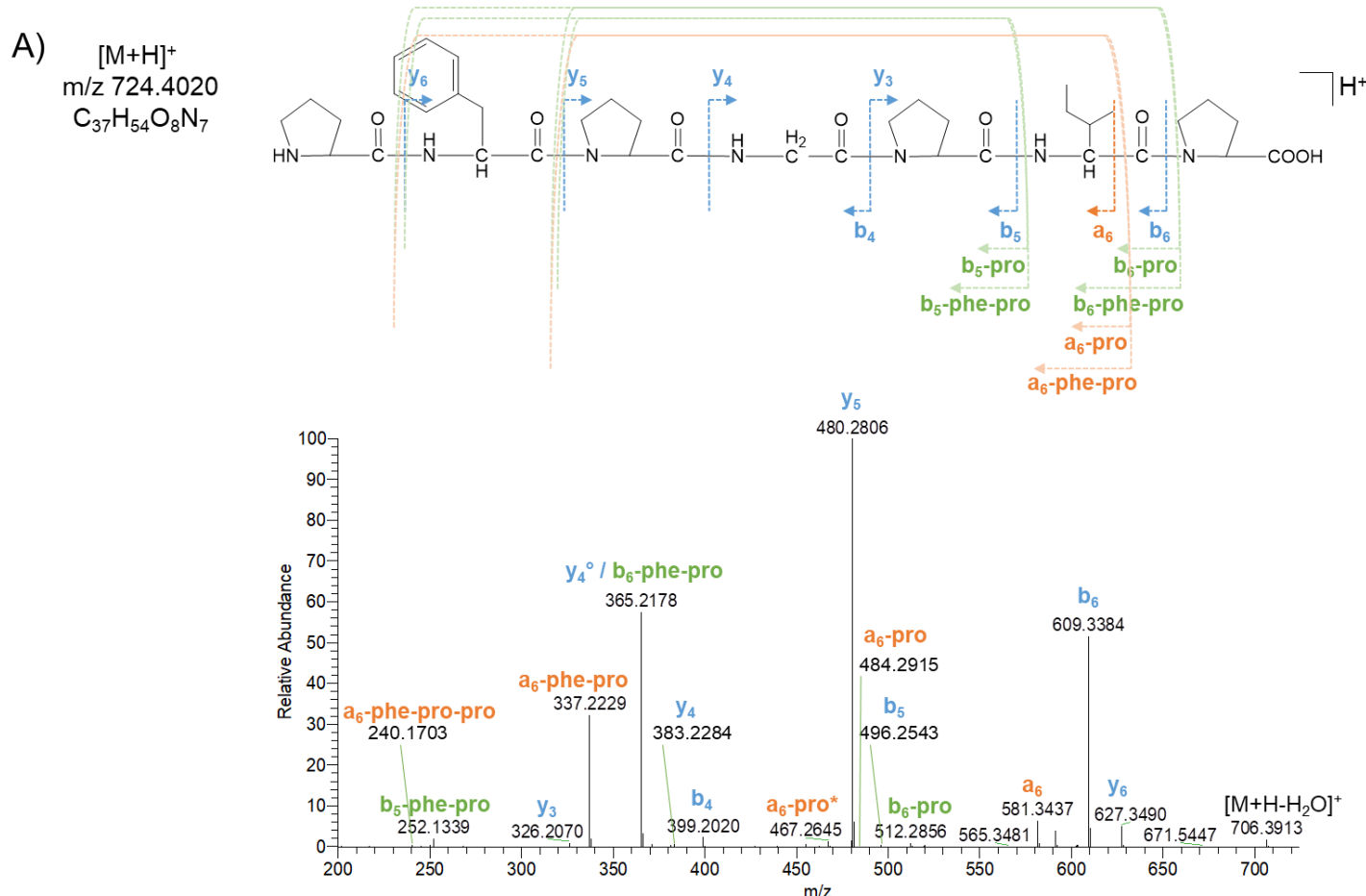


Figure S23. (A) HR-MS/MS spectrum of the $[M+H]^+$ pseudomolecular ion of compound 5 ($R_t = 17.4$ min). (B) HR-MS³ spectrum of the fragment ions a) and b) at m/z 365.2179 arising from fragmentation of compound 5. Ions marked with a circle (°) derive from the corresponding fragment after water loss; ions marked with an asterisk (*) derive from the corresponding fragment after NH_3 loss.

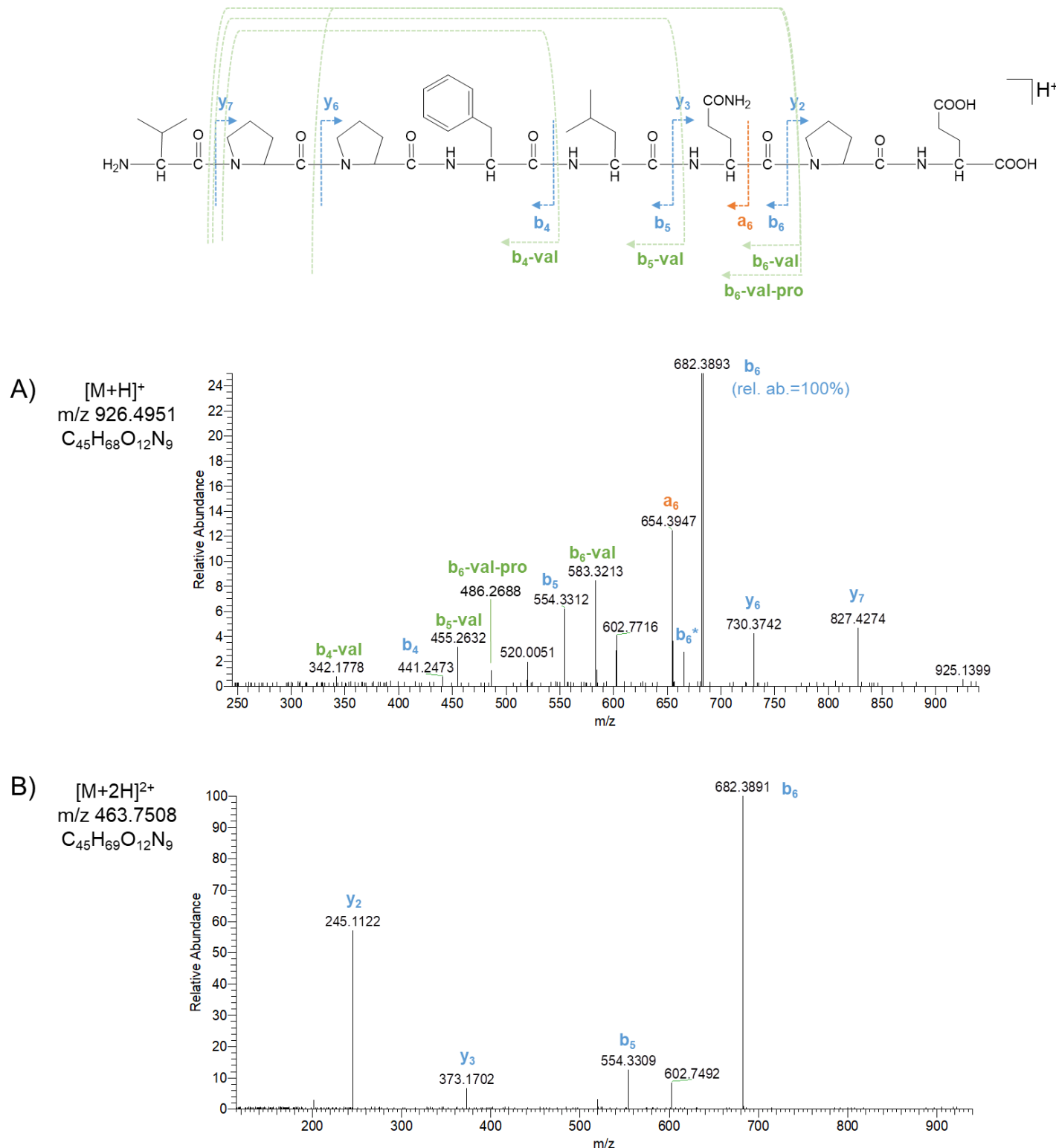


Figure S24. HR-MS/MS spectrum of the $[M+H]^+$ and $[M+2H]^{2+}$ ions of compound 6 ($R_t = 16.0$ min). Ions marked with a circle (°) derive from the corresponding fragment after water loss; ions marked with an asterisk (*) derive from the corresponding fragment after NH_3 loss.

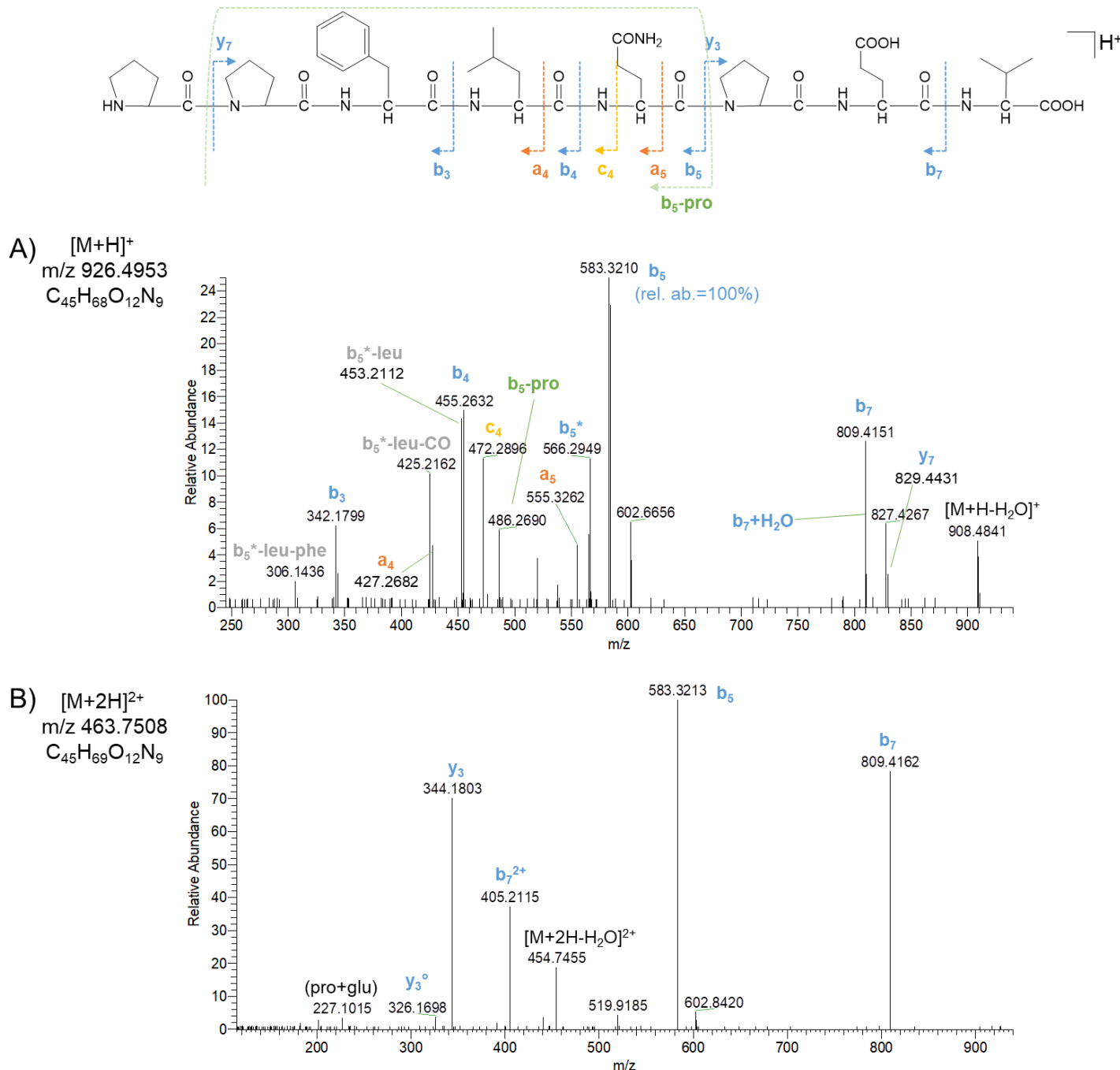


Figure S25. HR-MS/MS spectrum of the $[M+H]^+$ and $[M+2H]^{2+}$ ions of compound 7 ($R_t = 17.0$ min). The b_5^* ion (A) is expected to form a macrocyclic intermediate, presumably deriving from head-to-side chain cyclization between the N-terminal Pro and the Gln side chain, with concomitant NH_3 loss. This intermediate functions as a precursor to the formation of non-native, or scrambled, product ions (highlighted in grey). Ions marked with a circle (°) derive from the

corresponding fragment after water loss; ions marked with an asterisk (*) derive from the corresponding fragment after NH₃ loss.

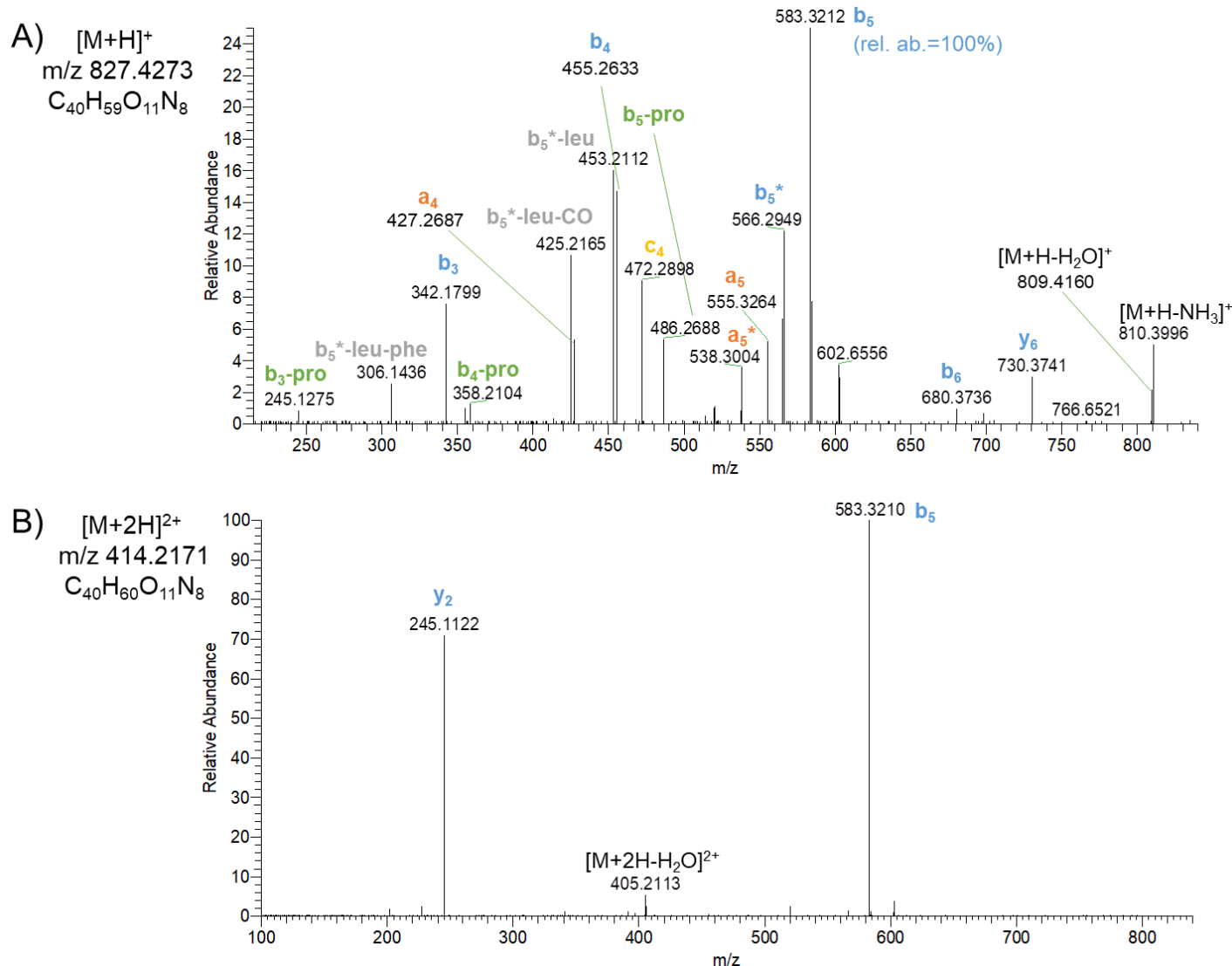
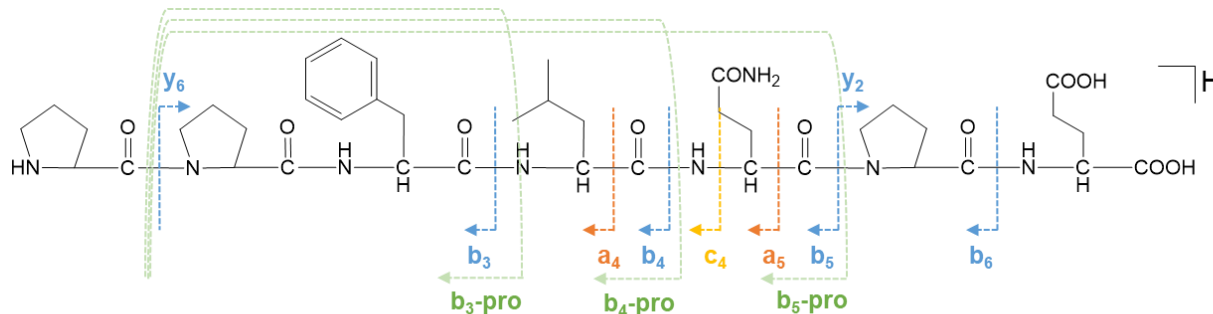


Figure S26. HR-MS/MS spectrum of the [M+H]⁺ and [M+2H]²⁺ ions of compound 8 ($R_t = 14.2$ min). The b_5^* ion (A) is expected to form a macrocyclic intermediate, presumably deriving from head-to-side chain cyclization between the N-

terminal Pro and the Gln side chain, with concomitant NH_3 loss. This intermediate functions as a precursor to the formation of non-native, or scrambled, product ions (highlighted in grey). Ions marked with a circle (\circ) derive from the corresponding fragment after water loss; ions marked with an asterisk (*) derive from the corresponding fragment after NH_3 loss.

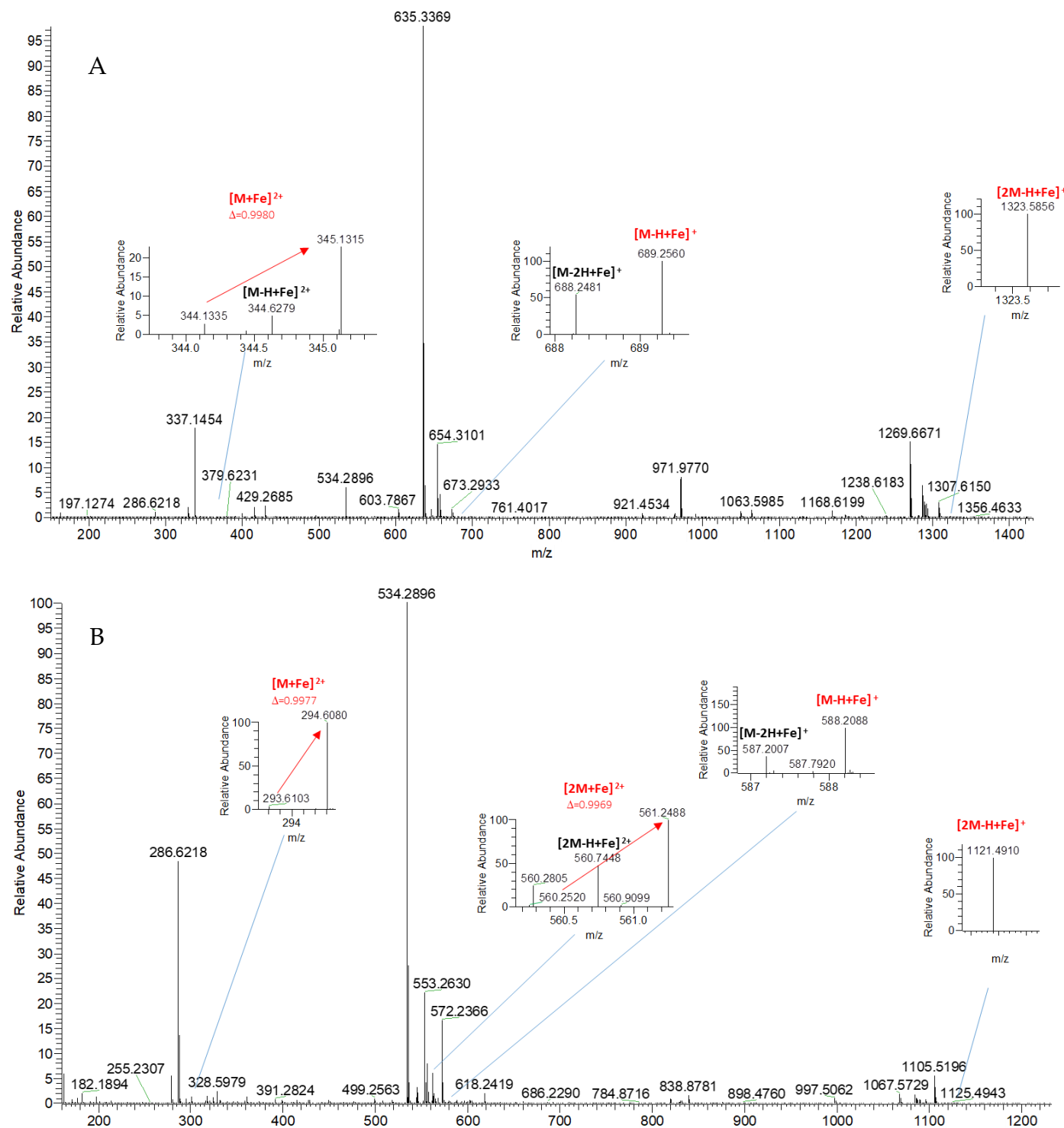


Figure S27. HRMS spectra showing iron adducts of compounds **1** (A) and **2** (B). Iron (II) adducts are depicted in red while iron (III) adducts in black. Where discernible, the typical mass difference between the two observable iron isotopes ^{56}Fe and ^{54}Fe was highlighted.

Table S3. Ferric reducing antioxidant power assay results of compounds **1** and **2**.^a

	compound 1	compound 2	Ascorbic acid
Abs 4 min (nm)	0.04	0.08	0.2
a.a. equivalents (μM)	21 ± 0	40 ± 1	-
FRAP value	41 ± 1	80 ± 2	-
Abs 16 min (nm)	0.05	0.12	0.2
a.a. equivalents (μM)	26 ± 0	60 ± 2	-
FRAP value	52 ± 2	121 ± 4	-

^aThe samples and controls were analysed at 593 nm in triplicates in order to infer the standard deviation, and the absorbance values reported were corrected for the blank reading (0.07). The results were compared with ascorbic acid 100 μM in order to calculate Ascorbic Acid (a.a.) equivalents values and in turn the FRAP values.

Peptidases from *Microbacterium* sp. V1

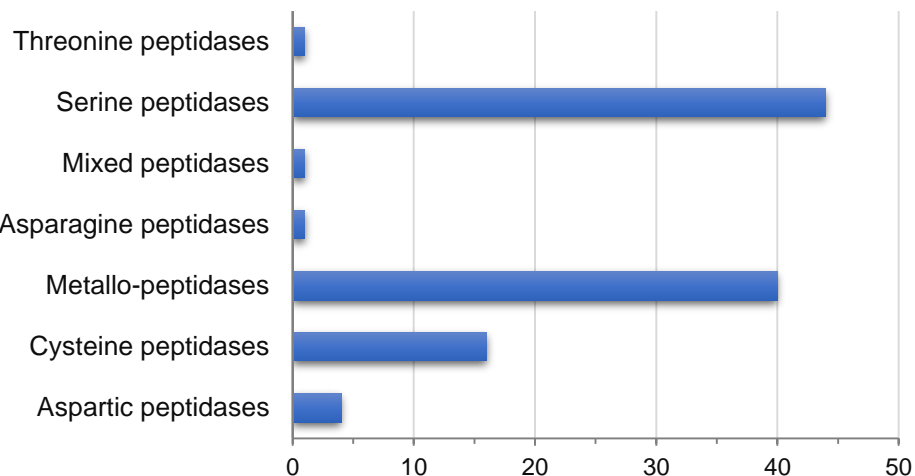


Figure S28. Peptidases from *Microbacterium* sp. V1 annotated by using the bioinformatic tool Hotpep-protease.